GERMAN - MONGOLIAN INSTITUTE
FOR RESOURCES AND TECHNOLOGY

The present work was submitted to
the German-Mongolian Institute of Resources and Technology

High-Altitude Drone Design: A Simulation-Based Approach for Extreme Atmospheric Conditions

Bachelor's Thesis

Submitted by: Belgutei Odgerel

Study program: Mechatronics engineering
Student ID: B2100109

1st Supervisor/Examiner: Ph.D. Odbileg Norovrinchen
2nd Supervisor/Examiner: Ph.D. Youngsuk Kim

Ulaanbaatar/Nalaikh

2025

GERMAN - MONGOLIAN INSTITUTE
FOR RESOURCES AND TECHNOLOGY

The present work was submitted to
the German-Mongolian Institute of Resources and Technology

High-Altitude Drone Design: A Simulation-Based Approach for Extreme Atmospheric Conditions

Bachelor's Thesis

Submitted by: Belgutei Odgerel

Study program: Mechatronics engineering
Student ID: B2100109

1st Supervisor/Examiner: Ph.D. Odbileg Norovrinchen
2nd Supervisor/Examiner: Ph.D. Youngsuk Kim

Ulaanbaatar/Nalaikh

2025

Statutory Declaration

Odgerel, Belgutei	B2100109
Last Name, First Name	Student ID Number

I hereby affirm in lieu of an oath that I provided the submitted bachelor thesis

High-Altitude Drone Design:

A Simulation-Based Approach for

Extreme Atmospheric Conditions

I did not use any sources other than those stated. In case that the work is additionally submitted on a data medium, I declare that the written and the electronic form are completely identical. The work was not submitted in the same or similar form to any examination authority.

Ulaanbaatar/Nalaikh, May 28, 2025	
Place, Date	Signature

Abstract:

Through the use of CFD (Computational Fluid Dynamics) simulation models, the study aims to conduct relative research between different drone designs and propulsion methods to find the ideal design for high-altitude near-space applications.

The research concluded that although each design had both advantages and disadvantages, the most ideal configuration for general application in extreme altitudes was the hexacopter, due to its powerful yet compact configuration.

The study also looked at different forms of thrust generation, assessing the efficiency, power, and range to determine the feasibility of their application in orbital regions. Overall, two of the three methods were operational in LEO (Low Earth Orbit) and above, confirming the feasibility of orbital drones.

Acknowledgments:

This section is dedicated to expressing my gratitude and acknowledging the works of all who have been instrumental in the creation of this thesis, either directly through the supervision and guidance or indirectly through inspiration and providing tools. I truly hope that my work can, in turn, be the foundation for future researchers to build their works off of, just as I have.

My deepest gratitude goes to my two supervisors, Prof. Odbileg and Prof. Kin Young Suk, whose expert advice and professional knowledge have not only guided me through my work but also provided invaluable feedback and corrected the flaws of my methods. This thesis would not be nearly as coherent and complete without their help.

I would like to express my sincere gratitude to Ansys Fluent and the developers for providing a free educational version for students to use. This tool has been the foundation upon which the majority of the research was built, providing accurate CFD simulations, which greatly enhanced the accuracy of the study. It has been an invaluable resource that was critical in the creation of this research.

Of course, major appreciation goes to the international research community, including NASA as well as individual researchers, which has provided unrestricted research to the whole global community. These researches have been instrumental in not only providing understandings of the topic but also finding the exact measurements required.

Lastly, my sincere gratitude goes towards the GMIT faculty, whose support has been invaluable in the completion of the thesis. They provided me with the resources, knowledge, and the opportunity to learn and expand my knowledge in a practical way.

Table of contents:

Chapter 1: Introduction

Overview:

As our technologies develop, becoming ever more sophisticated, we have made considerable advancements in space travel, starting the foundations of a thriving space industry. In 1957, with the launch of Sputnik 1 by the Soviet Union, the space age was officially kicked off. Shortly after, in 1958, NASA was established by the United States, which, in 1969, landed the first people on the moon with the infamous Apollo 11 mission. Today, many different national and international institutions, such as NASA, ESA, and CNSA, spearhead the development of the space industry, stationing rovers on both Mars and the Moon. Moreover, private entities such as SpaceX, founded by Elon Musk, and Blue Origin, founded by Jeff Bezos, are developing ever more efficient rockets on their mission to colonize Mars and the Moon, respectively.

Currently, it costs NASA approximately $10,000 to $20,000 to launch just one kilogram into space. Although modern reusable rockets, such as those developed by SpaceX, have managed to lower the cost to $2,000 per kilogram, continuous repeated missions to space for the purpose of travel or clearing debris largely remain unviable. With the current rapid expansion of the space industry, there is a need for cheaper, faster, and more sustainable methods of reaching orbit and operating in space. These advancements could revolutionize a wide range of space-based activities. For example:

- Servicing and repairing satellites could dramatically extend their operational lifespans and reduce the need for costly replacements.
- On-orbit manufacturing and assembly may allow us to build large-scale structures like space stations or solar arrays in orbit without needing to launch them in one piece from Earth.
- Space-based search and rescue missions could assist astronauts, satellites, or even future space tourists in distress.
- Active removal of space debris is becoming critical to prevent collisions in increasingly crowded orbital zones.

A simple solution to these major problems could be the development of UAVs (unmanned aerial vehicles) or drones capable of operating in orbital space regions, eliminating the need for constantly launching rockets from Earth to solve simple issues. The UAVs would be remotely operated, eliminating the need for a pilot, and would be

capable of performing a wide range of tasks while in orbit, from taking measurements and photography to more complex tasks such as providing maintenance to satellites and clearing debris. A major advantage of the drones is that they would be able to explore and provide services in extremely perilous environments, which would otherwise be too dangerous or risky for humans to perform. Therefore, the drones are ideally suited for operation in space due to their flexibility and versatility in terms of both maneuvering and task variety. They offer quick response times as well as cost and safety, making them a critical step in the future of the space industry.

Problem statement:

As of now, there are no fully operational UAVs actively servicing missions in Earth's orbit. Despite the use of robotic arms and semi-autonomous systems in space applications such as on the International Space Station, the use of fully autonomous UAVs in conducting outer-space missions, such as satellite servicing and debris collection, is largely theoretical. This research aims to conduct a study determining the feasibility of these concepts through their design and operational requirements.

The development of such drones could revolutionize the space industry as a whole, reducing the cost and danger in space missions; however, the development of these drones brings specific challenges that terrestrial drones wouldn’t normally face. Since the main point of the drones is to reduce the cost of launching, the drones must stay in orbit for extended periods of time, ideally indefinitely. As a result, the drones must be able to mostly be self-sustaining and reliable, operating with very little need for visiting refueling or repairing stations.

As a result , when considering the design of these drones, efficiency is the most important factor, both in terms of weight, power, and fuel consumption. Weight is a major consideration in any flying vehicle design, but for orbital UAVs, weight optimization is vital, as every added gram will quickly deplete its already finite power supply. Power is also important, providing the UAV with ample force to not only maintain itself but also to maneuver efficiently and quickly to perform the required tasks. Finally, fuel optimization ensures that the UAV can stay as long as possible in orbit without needing to resupply, making it a critical consideration.

Aim:

The aim of this study is to develop a comprehensive mechanical model of various types of drones designed for use in space environments. We will focus on the physical structures of the drones, such as propulsion systems and overall

configuration, to assess the aerodynamic behavior of different UAV designs as well as the thrust generated by the drones and whether it would be sufficient for operation. Through this method the study will assess the feasibility and mechanical and physical limitations of the UAVs in space and near-space environments.

To achieve this, the study will make extensive use of ANSYS Fluent, a powerful computational fluid dynamics (CFD) simulation tool used extensively in the aerospace industry to accurately simulate fluid behavior. The CFD analysis will be able to help us determine the aerodynamic properties and critical flight parameters such as lift, thrust, drag, and pressures applied on the UAVs, allowing us to accurately simulate lower air densities, such as in space and near-space regions, which provides us with a base to perform deeper analysis.

The ultimate goal of this research is to identify the most ideal design, both mechanically and aerodynamically, for future space drone missions. The study will aim to contribute valuable data and design guidelines through the use of CFD simulations provided by ANSYS Fluent for the development and design of orbital UAVs capable of efficient and sustainable operations in near and deep outer-space environments.

Objectives:

For the purpose of variety and comparison, we will study 4 different types of UAVs: quadcopter, hexacopter, octocopter, and VTOL (vertical take-off and landing), which are the most common types of drones used today. Each of the drones provides different applications and diversity to the study through rotor number and arrangement as well as overall design, each affecting their maneuverability, lift capacity, and aerodynamic efficiency. Through this study we will determine the advantages and drawbacks of each design and which kind of drone is the best suited for space applications by simulating environmental conditions differing with altitude.

In addition to comparing drone configurations, the research will also investigate the performance of three different propulsion systems: traditional propeller-based thrusters, ion thrusters, and PLT (photon laser thrusters). All three methods of propulsion provide fundamentally different approaches for generating thrust; thus, the analysis of each of them will be critical in determining the most optimal form of flight. Propellers are the traditional form of propulsion widely used in aviation; they utilize the air to create thrust, and thus at higher altitudes, their efficiency tends to drop. In contrast, ion thrusters move themselves forward by using highly charged ions. Despite having little thrust, it is very effective, making it perfect for use in space. PLTs are an

experimental technique that generates very little thrust by using light as propulsion, which makes it appropriate for deep space missions.

Finally, using all the data gathered, the study will determine the effective operational zones by examining the propulsion methods in combination with each drone design configuration. The ultimate goal is to use the obtained data from the simulated space conditions and determine which configurations are most appropriate for specific mission profiles, be it search and rescue, transportation, or measurements. This thorough comparison will shed important light on the trade-offs and design factors that go into building space drones.

Research questions:

At the end of this study, the following questions will be thoroughly examined:

- How do drones operate in near-space and space regions?
- Which drone design and propulsion type are ideal for which range?
- What are the important parameters for the operation of orbital drones?

Scope:

The goal of the research is to determine how different mechanical designs of various drone configurations affect their function in near-space environments, considering reduced gravity and air pressure as well as extreme heat, which greatly affect the quality of the atmosphere. Therefore, the mechanical and physical aspects of drone operation in space-related environments will be the main focus of this study, including aerodynamics, propulsion mechanisms, structural design, and overall mechanical efficiency as important research topics. Since this is already a very broad topic, the study will not examine the electrical systems, material sciences, or economic feasibility in order to keep its scope narrow. The study intends to produce important insights into the drones' functional viability and optimization for space missions by focusing on their mechanical performance and physical behavior.

In scope:

- Aerodynamics analysis (Drag)
- Propulsion analysis (Lift)
- Weight consideration
- Environmental simulation
- 3D design and simulation

Out of scope:

- Electrical system design

- Material science considerations
- Economic feasibility

Chapter 2: Literature review

Overview of drone history:

Although drones are now widely associated with modern warfare and civilian applications, the concept of early UAVs began through military experimentation more than a century ago. Back in World War I, UAVs made their debut as a new advanced form of surveillance and transport, capable of breaching enemy lines without risking the pilot's life. Among the first pioneering the field was “Kettering Bug,” an autonomous missile designed to fly to a predetermined position before exploding, which laid the foundation for later UAVs. (1)

The development of later technologies in the 20th century, such as autonomous piloting, remote control, measurement and detection, and digital signal processing, made the drones far more advanced and sophisticated. After the unfortunate events of September 11th, 2001, UAVs became a critically useful tool used in all sorts of military applications, such as tracking and locating hostile entities and targeted strike operations as well as general surveillance. More importantly, a major point in UAV development was their widespread adoption into civilian usage, be it for measurements, agriculture, surveillance, or simple entertainment. (1)

Drones today come in many shapes and sizes, each differing in their application, from small to large, efficient to powerful. Drones are capable of carrying out a variety of tasks. From smaller consumer-grade drones, often used for photography and measurements, to large industrial drones capable of conducting search and rescue missions, with their power and endurance, drones have exploded in variety and application. Despite this, drones still have immense future potential in areas such as space exploration and extraplanetary research; thus, understanding the current state and the history of drones is essential for the future space industry. (1)

Current Research into High-Altitude Drone Applications:

Since the application of UAVs in high-altitude regions is such an intriguing field, there have been numerous recent research studies discussing their application and feasibility. High-altitude regions are far beyond the typical range of aerial vehicles, well

above the troposphere and into the stratosphere, above 12 km, where the air pressure and quality significantly decrease due to the lower air density and temperatures. These problems are the focus of the research, which will be discussed in this section, which will provide us with a deeper understanding of the field.

The study "Approach to Evaluation of the Application and Efficiency of Stratosphere UAV" offers one method for assessing the effectiveness and suitability of drones in the stratosphere. This study examines various approaches and identifies critical parameters to evaluate the theoretical performance of UAVs at extreme altitudes. It concludes that variables like power consumption, data transfer, and stability must be taken into consideration in addition to basic aerodynamic design. Furthermore, drone designs must be specifically made to adapt to the environment in order to maintain stable lift and thrust. (2)

Propeller design is a vital component of UAV performance, particularly at extreme altitudes, where the atmospheric conditions, importantly air density, drop considerably from those on the surface. In the study “Design and Optimization of a High-Altitude Long-Endurance UAV Propeller,” these conditions were investigated by the researchers using computational fluid dynamics (CFD) and design-optimizing algorithms in order to determine the aerodynamics of the drones and the efficiency of the propellers in stratospheric operation. They found propeller designs capable of generating sufficient thrust up to 22 km. (3)

By examining the viability of using proton-exchange membrane (PEM) fuel cells to power drones and identifying the important factors to consider when integrating fuel cells into UAVs, the study "Design of an Unmanned Aircraft System for High-Altitude 1 kW Fuel Cell Operation" further expands on UAV capabilities at high altitudes of 10–11 km. This provides an alternative to solar energy, which becomes crucial for conducting continuous extended missions where an ample supply of sunlight is not always guaranteed due to weather and night cycles. (4)

“Towards the Advent of High-Altitude Pseudo-Satellites (HAPS)” is research that provides a multidisciplinary view of high-altitude drone platforms, which can provide cost-effective, reusable, and stable solutions for surveillance, monitoring, and communications as well as emergency response. The study also discusses the technical, operational, and design challenges of these pseudo-satellites, which would be a vital part of space UAV development, bridging the gap between satellites and drones. (5)

Together these studies outline the current advancements and limitations of research into UAVs, particularly in high-altitude regions, which highlight the current trends and will become the stepping stones from which the next generation of

aerospace vehicles will be developed. Likewise, this research will be heavily based on the findings of the discussed research to create more well-informed assumptions.

Theory Behind Mechanics of Flight

The basic aerodynamic forces that influence each aerial vehicle's performance and properties are lift, weight, thrust, and drag; thus, the design of not only UAVs but all aircraft must carefully balance all these forces in order to ensure stable and controlled flight. Thus, to analyze the efficiency and performance of the UAVs, we must have an understanding of the physics behind flight mechanics as well as the factors that contribute to it.

Lift: (6) Lift is the most fundamental force of aviation, which allows aircraft to levitate despite the influence of gravity, in most cases, though not always, utilizing wings or rotors to accelerate air, pushing it down to produce an equal and opposite force utilizing Newton's third law. Fixed-wing aircraft generate lift by pushing air under their aerofoil-shaped wings, creating a pressure difference, whereas rotor-based aircraft, like helicopters and drones, produce lift by sucking air and accelerating it downwards.

When calculating the lift, the following parameters should be carefully considered:

- The shape and structure of wings
- Air density and temperature
- The speed of the air over the surface

Weight: (6) Simply put, weight is the force that gravity applies to the vehicle, which lift must overcome in order to lift off and keep the vehicle in stable flight. Weight must be kept to a minimum without sacrificing the vehicle's structural soundness because any additional weight creates more lift, which significantly lowers flight efficiency. For weight, it's important to consider:

- Using lightweight, strong materials
- Distribute weight evenly
- Accounting for payload which influence the center of gravity

Thrust: (6) The force produced by the propulsion method of the aircraft, either engines, jet turbines, or propellers, to move and control the vehicle is thrust. Aircraft maneuver themselves using thrust to control their speed and angle, allowing them to move freely in pitch, roll, and yaw using control surfaces such as elevators, rudders, and ailerons. Moreover, depending on the orientation and positioning of the thrusters, it can also be used to produce lift, like in rotor-based vehicles.

The following parameters are vital for thrust:

- Engine output power

- Propeller or turbine characteristics
- Fuel type and efficiency

Drag: (6) When moving at a given speed, a certain amount of force called drag is induced because of the air being pushed and providing friction on the aircraft. Drag is almost always undesired; thus, increasing efficiency requires minimizing drag, which is done through the implementation of smooth, streamlined design. Having less drag can greatly reduce energy requirements and increase aircraft speed.

The forms of drag include:

- Parasitic drag from protruding elements
- Induced drag from vortices
- Form drag of the shape and structure

Aerodynamics: (6) The behavior of air interacting with and flowing around the aircraft is referred to as aerodynamics, and it is a vital part of determining the characteristics of the system. Aerodynamics can be greatly influenced by properties of the air and structure of the vehicle; thus, aerodynamic design greatly helps to improve the overall efficiency of the system through a streamlined structure, which minimizes drag and maximizes lift and thrust. Aerodynamics can be affected by:

- Wing shape and structure
- Surface deflection
- Flow separation
- Effects of turbulence

Drone-Specific Flight Mechanics

Drones and conventional aircraft both adhere to the basic rules of flight. Weight, drag, lift, and thrust. Because of their special configuration and operating needs, drones introduce unique mechanical behaviors. For example, multirotor drones accomplish control by modulating the speeds of individual rotors, in contrast to traditional aircraft, which depend on aerodynamic surfaces like wings, rudders, and elevators for stability and

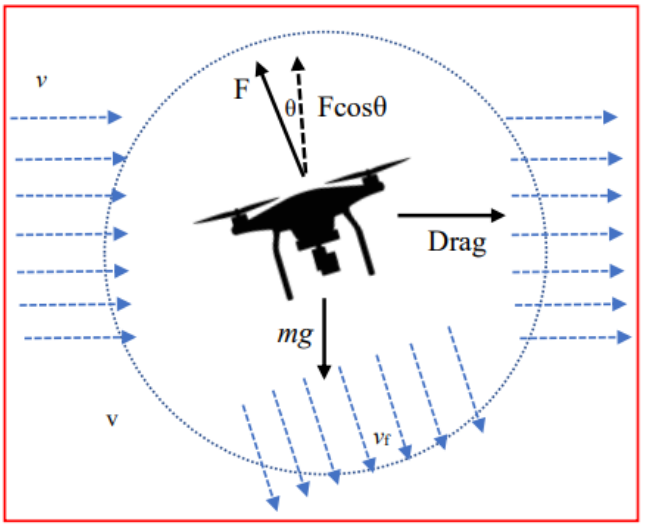

Figure 1. Drone flight illustration

maneuverability. Drones can modify their pitch, roll, and yaw without the use of intricate mechanical control surfaces by varying the thrust of particular motors. This dynamic thrust vectoring technique offers remarkable agility, allowing for accurate hovering and quick positional changes. This is especially useful in confined spaces or during takeoff and landing procedures. (7)

The dependence on advanced onboard flight control systems is a crucial aspect of drone performance, allowing the incorporation of various sensors, including inertial measurement units, barometers, magnetometers, and GPS, to continuously monitor the drone's orientation, altitude, and location. In order to stabilize the drone, adjust for disruptions like wind or payload shifts, and accurately carry out user or autonomous commands, the data is processed in real time. (7)

The efficiency of flight is also significantly influenced by propeller design, as small, fast rotors with blade geometries tailored for low Reynolds number situations are commonly found in drones. Thrust generation and noise levels are directly influenced by the number, pitch, and diameter of the propellers. Additionally, designers need to take into account the possibility of aerodynamic interference between rotors, particularly in small multirotor configurations. (7)

Due to their open structures and parts that produce parasitic drag, the majority of drones are not naturally aerodynamic. This has led to the development of hybrid platforms, such as VTOL aircraft, which combine the effective forward motion of fixed wings with the vertical lift potential of rotors. These designs are especially well-suited for high-altitude or long-range missions where aerodynamic efficiency is crucial.

Overview of Propulsion Methods:

Throughout this study, we model three different propulsion system types that may be useful for drone operations, especially in near-space and high-altitude settings. These propulsion techniques are PLT propulsion, ion thrusters, and propeller-based systems. Each of these technologies has distinct benefits and drawbacks, particularly when used in low-density or vacuum-like atmospheric conditions, functioning on essentially different physical principles. The purpose of this section is to give a thorough explanation of each propulsion system's operation, the physics underlying its thrust generation, and its suitability for various flight regimes.

Propeller-based propulsion

The primary and most basic method of thrust generation in aviation is propeller-based propulsion. Propellers are the main component that transforms

mechanical energy into thrust in a variety of devices, including small drones, general aviation aircraft, unmanned aerial vehicles (UAVs), and even some hybrid high-altitude systems. They are a key component of contemporary flight technology due to their comparatively straightforward design, high efficiency at lower speeds, and versatility across a variety of platforms. Therefore, in practically every area of aerospace and aeronautical engineering, it is crucial to comprehend their design and function. (8)

Number of Blades:

A propeller's total efficiency is only slightly impacted by the number of blades on it. Increasing the number of blades generally results in marginally better performance because the power and thrust produced are dispersed more evenly throughout the airflow. This can result in improved control and more seamless operation, particularly in a variety of flying circumstances. (8)

Velocity:

The required pitch distribution across the blades is determined by the propeller's rotational speed (RPM) in conjunction with the incoming airspeed. Propellers with a high pitch angle may function well at the speed for which they were intended, but they may encounter issues like aerodynamic stalling when exposed to high axial flow rates. This emphasizes how crucial it is to adjust pitch for all operational circumstances, not just maximum effectiveness. (8)

Diameter:

A key factor in determining aerodynamic performance is propeller diameter. Because larger propellers engage a larger volume of air, the thrust and power can be distributed over a larger area, making them generally more efficient. At lower rotational speeds, this enhances thrust generation and minimizes energy losses. (8)

Fluid Density:

Fluid density does not directly affect a propeller's efficiency, but it does have a big impact on the size and shape of the blades. Because thrust and power are proportional to fluid density, propellers used in denser media (like water) are typically much smaller than those used in air. Moreover, in high-speed applications such as aeroplane propellers, low pressure at the blade tips may produce supersonic flow regions. (8)

Thrust:

The amount of fluid a propeller accelerates per unit of time, the acceleration rate, and the medium's density all affect the thrust it produces. From the standpoint of momentum, this relationship can be stated as follows: (8)

$$T = \frac{\Pi}{4} \cdot D^2 \cdot \left(v + \frac{\Delta v}{2}\right) \cdot \rho \cdot \Delta v$$

(1)

T = Thrust (N)

D = Propeller diameter (m)

v = Velocity of incoming flow. (m/s)

∆v = additional velocity, acceleration by propeller. (m/s)

ρ = Density of fluid. (kg/m³)

Ion thrusters:

An alternate propulsion method is needed because conventional propellers, which rely on the earth's atmosphere, cannot operate in space. For this purpose, ion thrusters stand out for their effectiveness, ability to precisely control thrust, and suitability for extended spaceflight. They work by ionizing a neutral gas, usually a noble gas like xenon, and then using an electric field created between a number of electrostatic grids to accelerate the ions that are produced. According to Newton's third law, the ejected ions create momentum, which provides thrust in the opposite direction.

The research “Development and test of a cost-efficient gridded ion thruster propulsion system for small satellites—IonJet” discussed the feasibility of the IonJet gridded ion thruster, which is intended for economical operation on small satellites and represents a noteworthy breakthrough in this area. The increasing demand for small, effective propulsion systems that work with drones and other small satellite platforms is addressed by this work. The modular and power-efficient design of the IonJet system reduced overall system complexity while preserving performance metrics. (9)

In the study, the following formula was used to describe the thrust:

$$T_i = I_b \sqrt{\frac{2m_i(U_b + U_p)}{q_0}} \qquad (2)$$

T_i = Thrust (N)

I_b = Ion beam current (A)

m_i = Ion mass (kg)

U_b = Beam voltage (V)

U_p = Plasma potential (V)

q_0 = Elementary charge (C)

Both krypton and xenon were used as propellants in the system's testing. Because of its high atomic mass and advantageous ionization properties, xenon is the conventional choice for ion propulsion; however, krypton is being investigated as a less expensive option. For missions with less stringent delta-v requirements, the study shows that krypton can still deliver usable thrust levels despite its reduced performance.

Photon Laser Thrusters (10)

A new class of spacecraft propulsion systems called photon-based propulsion systems produces thrust without the use of conventional propellant; rather, it depends on the physical fact that light has momentum and that photons, when emitted or reflected, apply a tiny but detectable force to the object in question. This force can be used to alter a spacecraft's velocity over time or with enough intensity, which makes it particularly appropriate for formation flying, deep space missions, and precise orbital adjustments.

The Photonic Laser Thruster (PLT) is one of the most exciting ideas in this field. The PLT is a propulsion system that uses a recycled laser beam inside a high-finesse optical cavity to greatly increase the momentum exchange from photons. The PLT traps photons between mirrors, bouncing them back and forth hundreds or even thousands of times instead of letting them reflect just once. By using multiple reflections, the spacecraft can receive a substantially larger total momentum than it would from a single reflection, which increases thrust without requiring onboard propellant.

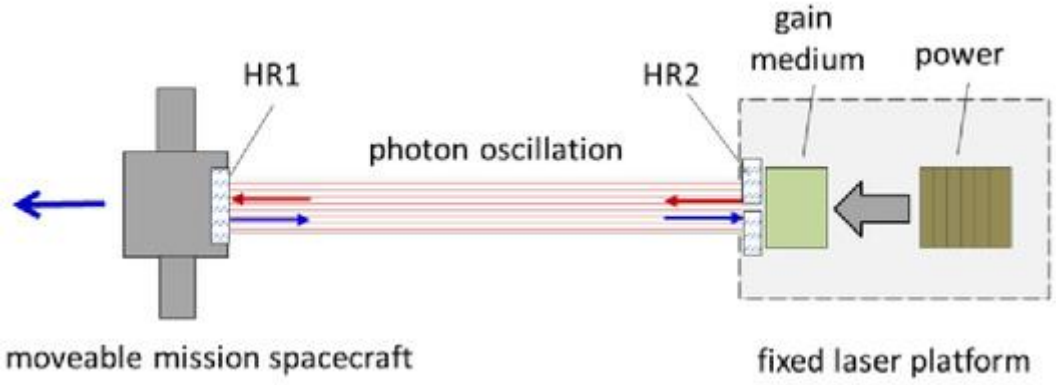

Figure 2: Photon laser thruster diagram

In the study "The theory modelling analysis of photonic laser propulsion based on oscillation in external cavity," a thin-disc laser and highly reflective mirrors were used to illustrate the system. By increasing the number of photon bounces and the laser power, the test setup demonstrated that thrust could be scaled up. The study

discovered that with a 1 kW laser, mirrors with a reflectivity of 0.99999, and a cavity length of 10 meters, the system could reach a maximum thrust amplification factor of 500,000 under perfect circumstances, where all incoming photons are completely absorbed within the optical cavity without escaping. A peak photon thrust of 0.333 N would be produced by this configuration, which is adequate to satisfy the needs of space mission applications. (10)

The thrust generated by the PLT is modelled by the following equation:

$$F_t = (1 + r_1)\frac{W_{eq}}{c}$$

(3)

F_t is the total thrust generated (N)

W_{eq} is the laser power (W)

c is the speed of light (m/s)

r_1 is the reflectivity of the mirrors in the optical cavity.

Environmental design:

We use the Jacchia-Bowman 2008 (JB2008) and the U.S. Standard Atmosphere 1976 (US76) models to estimate upper-atmospheric conditions at high altitudes. We can produce precise, altitude-dependent profiles of air density and viscosity over the entire range of orbital altitudes by combining these two models, using US76 for the lower atmosphere and JB2008 for the upper atmosphere.

Up to an altitude of about 1,000 km, the U.S. Standard Atmosphere model (often referred to as US76) offers a static, globally averaged vertical profile of atmospheric characteristics like pressure, temperature, density, and viscosity. It functions as a baseline model for common engineering computations and is based on historical meteorological data, especially at low to mid-altitude ranges. (11)

For higher altitudes, particularly above 90 km, where atmospheric characteristics differ greatly depending on solar activity, geomagnetic conditions, and time of day, the Jacchia-Bowman 2008 (JB2008) model is a dynamic thermospheric model. JB2008 is better suited for drag modelling in precise orbit determination and for simulating realistic atmospheric density in upper-atmospheric regions because it takes solar flux and geomagnetic indices into account. (12)

Air density:

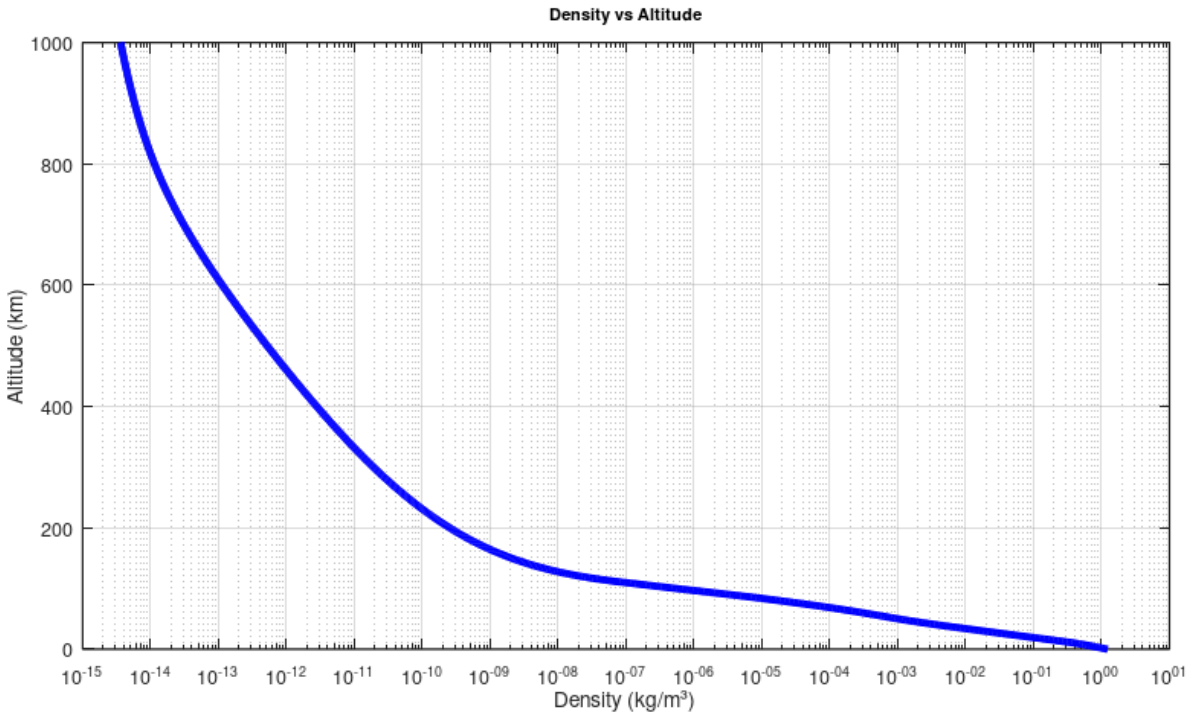

Figure 3. Air density dependent on altitude graph

Air density is highly dependent on altitude, decreasing exponentially as one moves away from the Earth's surface, as the US76 atmospheric model makes evident. Air density is around 1.225 kg/m³ at sea level, but because of the decreasing weight of the air above and the decreased atmospheric pressure, this value rapidly decreases with altitude. Commercial aircraft normally fly within the first 10 kilometers, where the air density already drops by almost two-thirds. The density is less than 1% of its sea-level value by the time the altitude reaches 50 kilometers. This sharp decline persists into the upper atmosphere, where conventional aerodynamic principles start to fail due to extremely low densities that cause air molecules to be widely separated. Exponential and piecewise polynomial relationships based on temperature gradients and pressure changes in each atmospheric layer are used in the US76 model to represent this behavior.

Viscosity:

One important factor affecting fluid motion, viscosity, is strongly influenced by temperature. Liquids typically become less viscous as the temperature rises, whereas gases become more viscous as the temperature rises. The fluid's molecular interactions are the cause of this behavior. Higher temperatures in liquids weaken intermolecular cohesion, which permits molecules to flow more freely and lowers flow

resistance. On the other hand, higher temperatures in gases raise the average kinetic energy of molecules, causing more frequent and forceful collisions that raise internal friction and, consequently, viscosity.

The Sutherland formula is frequently used to measure the relationship between temperature and gas viscosity. For ideal gases at various temperatures, this empirical equation gives a reasonably accurate estimate of dynamic viscosity. The formula is given as:

$$\mu = \mu_0 \left(\frac{T}{T_0}\right)^{\frac{3}{2}} \left(\frac{T_0 + C}{T + C}\right) \tag{4}$$

μ is the dynamic viscosity at temperature T

μ_0 is the reference viscosity at temperature T_0

C is Sutherland's constant

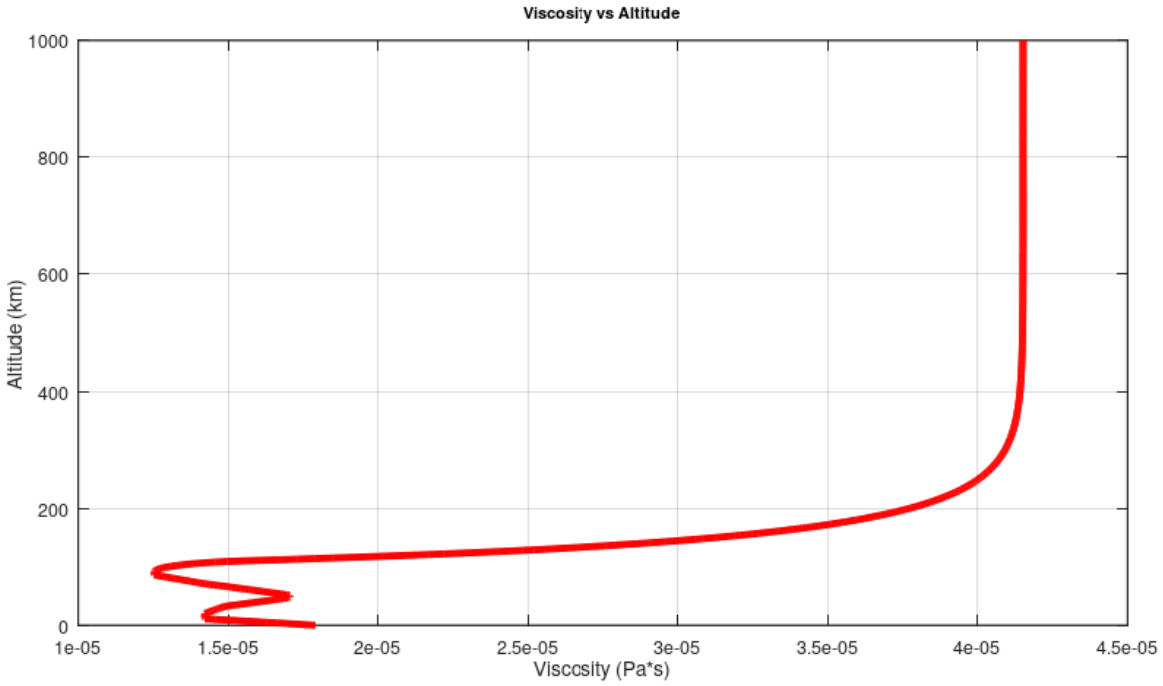

Figure 4. Viscosity dependent on altitude graph

The temperature at a specific altitude is calculated using US76. Sutherland's formula can be used to precisely determine the dynamic viscosity of air once the precise temperature at a desired altitude has been determined. We observe that the overall trend of viscosity in the atmosphere is nonlinear, even though the temperature decreases at lower altitudes. For example, the dynamic viscosity of air decreases slightly as the temperature drops up to about 11 km, the tropopause. However, the

viscosity rises in tandem with the temperature in the stratosphere, the uppermost layers of the atmosphere, where the temperature starts to rise once more with altitude.

Gravity:

Since gravity directly affects the stability, trajectory, and propulsion needs of orbital drones, it is essential to their development and operation. For any object in orbit to stay aloft and perform efficiently, gravity must be continuously resisted. Thus, for precise modelling and control, it is crucial to comprehend how gravity varies with altitude. A plot of gravitational acceleration versus altitude makes it evident that gravity gradually decreases as altitude increases. Usually, the curve exhibits a gradual but steady decrease, particularly in the first few hundred kilometers above the surface of the Earth. This is due to gravity being inversely proportional to the square of the distance from the center of the Earth, as described by the formula:

$$g = \frac{GM}{(R+h)^2} \tag{5}$$

g is the gravitational acceleration (m/s²)

G is the universal gravitational constant (Nm²/kg²)

M is the mass of the Earth (kg)

R is the mean radius of the Earth (m)

h is the altitude above the Earth's surface (m)

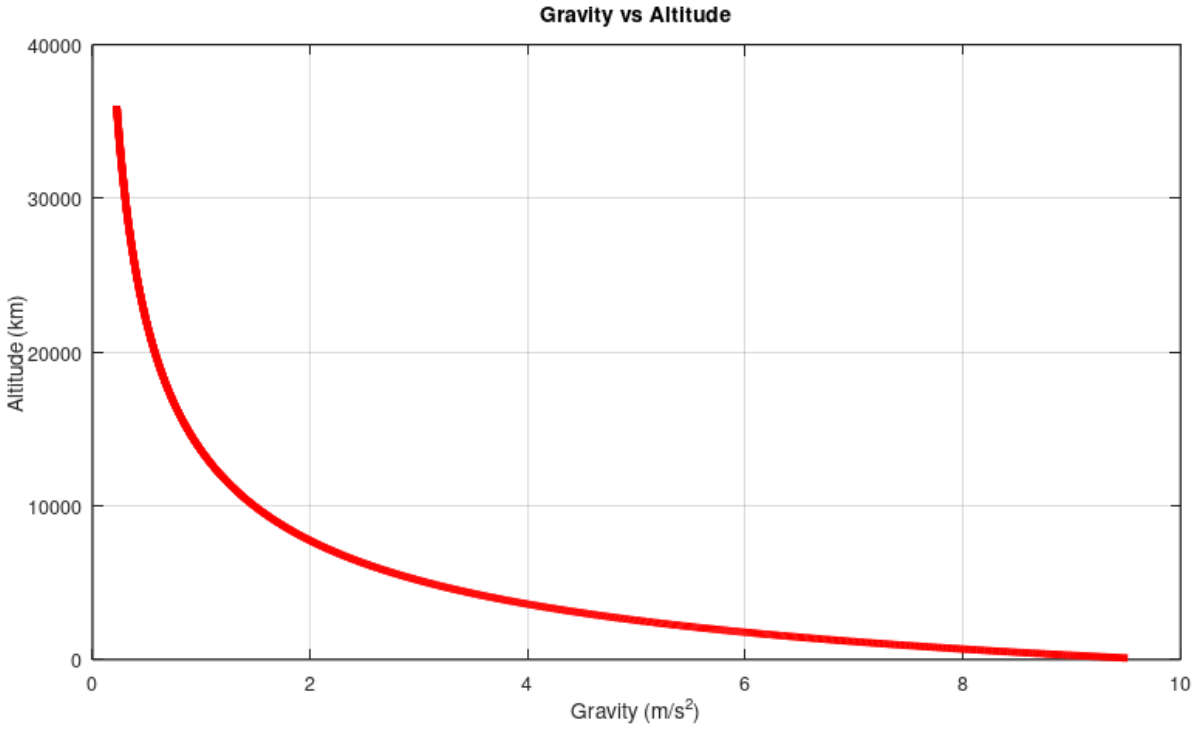

Figure 5. Gravity dependent on altitude graph

Chapter 3: Methodology

This study uses both theoretical design and computational simulation in a methodical manner to investigate the effectiveness and performance of different drone configurations. Based on their structural variations and usefulness for aerial operations, four different drone types—quadcopters, hexacopters, octocopters, and VTOL systems—have been chosen for in-depth examination. Every drone model will be created with consideration for mechanical elements like aerodynamic profile, structural layout, and rotor arrangement. In order to evaluate their effects on drone behavior in various flight regions, especially in high-altitude or near-space environments, the study also takes into account the three main propulsion techniques that were previously discussed: propeller-based, ion thrusters, and photon-based propulsion. ANSYS Fluent will be used to build a thorough simulation environment for assessing aerodynamic performance, stability, and efficiency in controlled settings. Based on accurate environmental data, this entails establishing boundary conditions, meshing techniques, flow models, and material properties. The outcomes of the simulation will serve as the foundation for performance benchmarking and design optimization by comparing the operational range and suitability of each drone type for various aerospace missions.

Drone design:

Each drone type is broken down in detail in this section, along with information on its rotor configurations, functional design logic, and geometrical dimensions. Arm lengths, propeller sizes, body shapes, and symmetry were all meticulously crafted for each configuration to replicate their real-world counterparts while preserving consistency for comparative analysis. The APPENDIX will contain the precise engineering schematics for every design.

Quadcopter:

Quadcopters, also known as quadrotor drones, are among the most popular and extensively utilized configurations in the design of UAVs. In order to balance torque and preserve stability, they are made up of four rotors arranged in a symmetric cross configuration, usually with two rotating clockwise and two anticlockwise. Quadcopters are perfect for both industrial and recreational applications because of their high degree of manoeuvrability, precise control, and mechanical simplicity. Without the need for intricate control surfaces, the vehicle can hover, perform vertical takeoff and landing,

and move nimbly in midair by adjusting the speed of individual motors to provide thrust and directional control. Quadcopters are particularly well-suited for low- to mid-altitude operations because of their comparatively small size and effective lift distribution. In this study, the quadcopter serves as a baseline model to compare performance and efficiency to more complex configurations like VTOL systems, hexacopters, and octocopters, particularly in high-altitude or near-space environments.

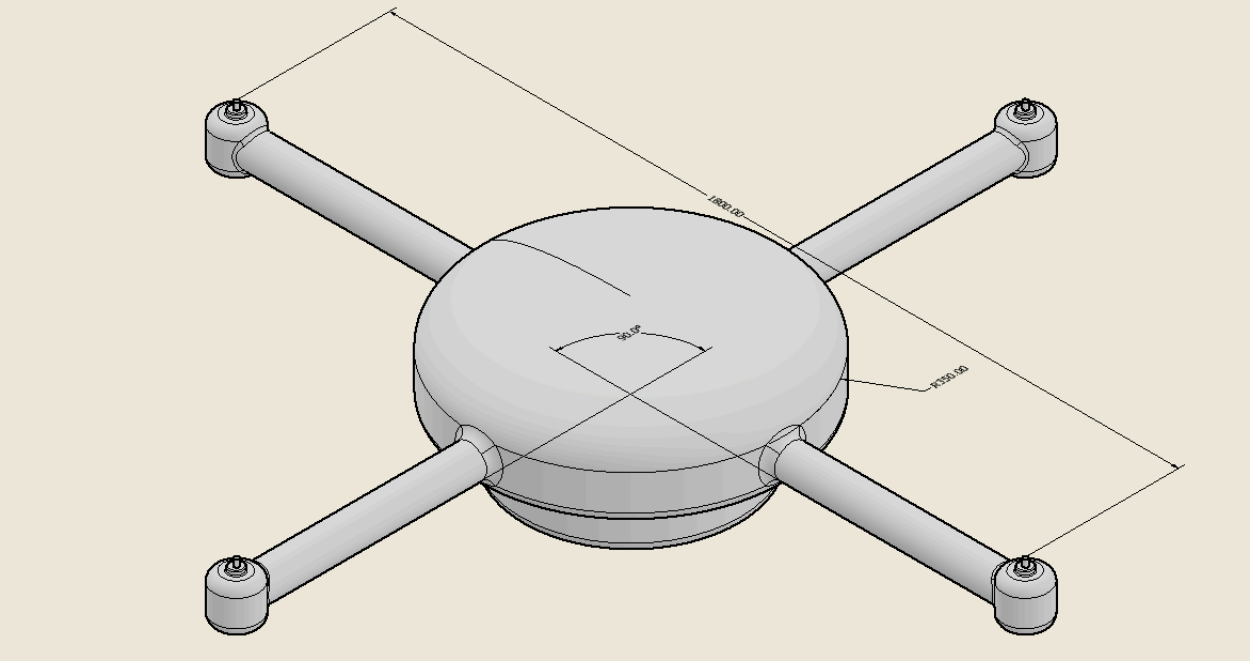

Figure 6. Quadcopter 3D design

The drone is made up of 2 main parts: the main body and 4 arms. The drone is radially symmetrical, each arm being positioned at exactly 90 degrees from each other. In total, the drone is 1.8 m long, most of the length being in the arms; at the end of each, the propulsion is located. However, the main body, having a radius of 35 cm, contains most of the surface area and mass. The drone in total has a volume of 0.106 m^3.

Carbon fiber is the ideal material because of its remarkable strength, weight, and durability balance, allowing drones to minimize total mass while maintaining structural integrity thanks to their high strength-to-weight ratio. Assuming the drone has an average frame thickness of 4mm (average drones range between 2 and 3 mm, and industrial drones range from 4 to 6 m) and the density of carbon fiber is approximately 1750 kg/m^3, we can calculate the mass of the frame using the square-cube law, which would be 2.333 kg.

Hexacopter:

A hexacopter is a class of multirotor UAVs with a central frame and six rotors arranged symmetrically. Compared to conventional quadcopters, this arrangement has a number of significant benefits, such as enhanced lift capacity, stability, and redundancy, with six motors increasing operational reliability, particularly in remote or high-risk environments, by allowing for better load distribution and allowing the drone to maintain controlled flight even in the event of a motor failure. Additionally, hexacopters have more thrust and payload capacity, which makes them appropriate for transporting larger items like sophisticated sensors, cameras, or scientific instruments. Because of their sturdy construction, hexacopters are frequently employed in fields like environmental monitoring, search and rescue missions, and aerospace research that call for greater endurance, greater altitudes, or precise manoeuvrability.

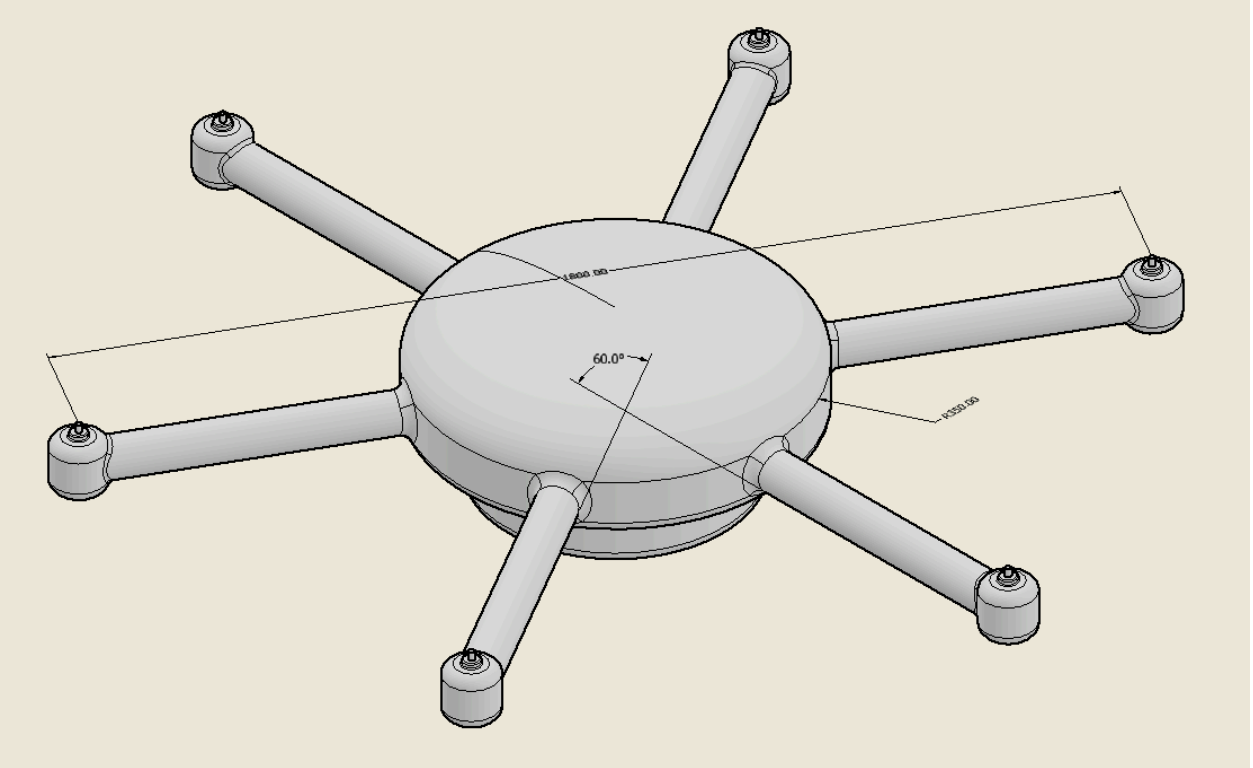

Figure 7. Hexacopter 3D design

Similar to the quadcopter, the hexacopter drone is made up of 2 main parts. The main body is identical to the quadcopter, but it has 6 arms arranged at 60 degrees from each other. This drone is also 1.8m long; however, due to the added arms, the volume is greater at 0.112 m^3. Again assuming a thickness of 4mm, the mass of the frame would be 2.465 kg.

Octocopter:

Octocopters are UAVs with eight rotors, making them one of the most powerful and stable multirotor drone configurations. Octocopters, which have eight uniformly spaced motors, offer remarkable lift capacity, flight stability, and redundancy, which make them perfect for demanding applications where performance and safety are crucial. In addition to improving control responsiveness, the vehicle's increased rotor count enables it to transport larger payloads more effectively. Octocopters can continue to fly in a controlled manner even if one or both of their motors fail, which is crucial for mission-critical tasks like professional cinematography, aerospace testing, industrial inspections, and high-altitude scientific research. Octocopters excel in precision flight, load balancing, and resilience, making them a prime candidate for advanced drone applications in both terrestrial and near-space environments, despite requiring more energy and sophisticated control systems than smaller multirotors.

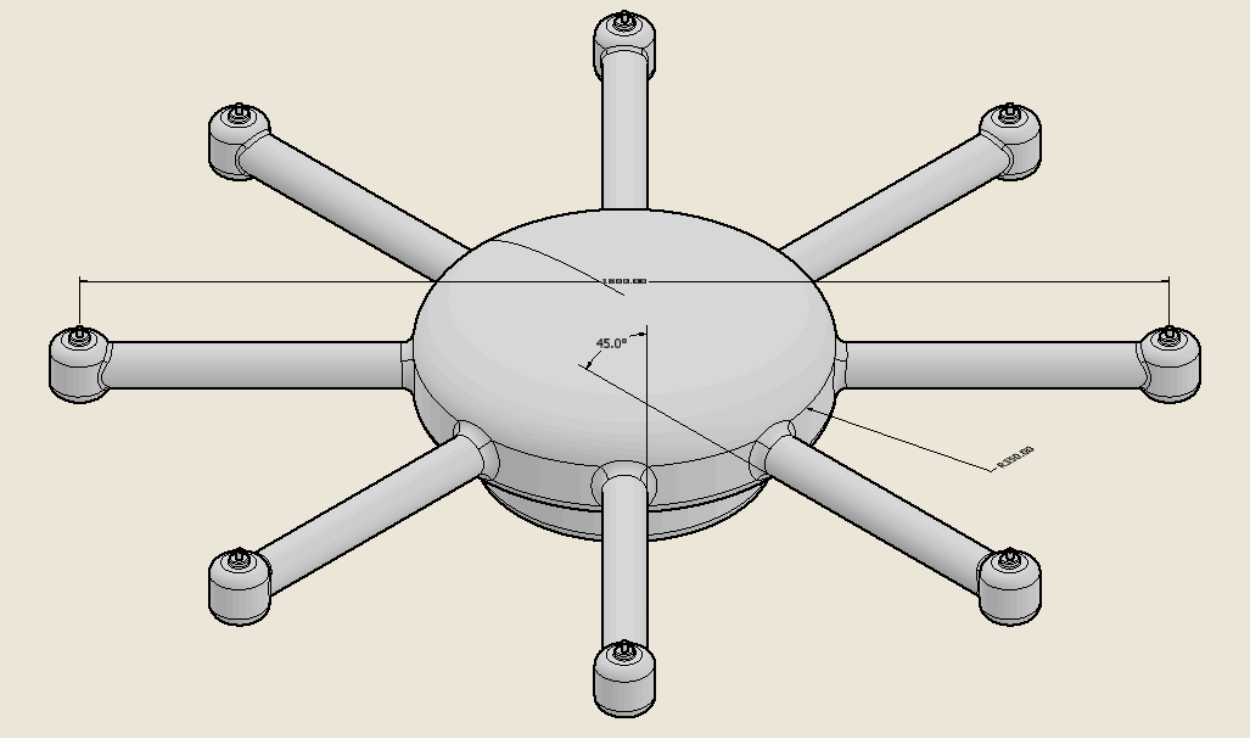

Figure 8. Octocopter 3D design

The Octocopter, similar to the previous 2, is another radially symmetrical drone, which has 8 arms 45 degrees apart from each other. The main body is also 35 cm with a total length of 1.8 m; it has a total volume of 0.118 m^3. Assuming it is once again made of carbon steel with a thickness of 4 mm, this frame weighs 2.597 kg.

VTOL Drone:

Vertical Take-Off and Landing (VTOL) drones represent a class of aerial vehicles that combine the aerodynamic efficiency of fixed-wing aircraft with the vertical lift capability of multirotor systems. Without the need for runways, VTOL drones can take off, hover, and land in tight areas while maintaining long-range, energy-efficient forward flight while cruising thanks to their dual-mode operation. Because of their versatility in launch and recovery operations, VTOL systems are particularly useful in aerospace and high-altitude research, making them appropriate for harsh or remote environments. For seamless transitions between flight modes, these drones frequently have tilting motors or independent lift and cruise propulsion systems. VTOL drones are perfect for missions like collecting atmospheric data, satellite servicing concepts, and exploration missions in Earth's upper atmosphere and other planetary bodies, despite having a more complicated mechanical design than traditional quadcopters or fixed-wing drones. These drones also offer significant advantages in range, endurance, and payload capacity.

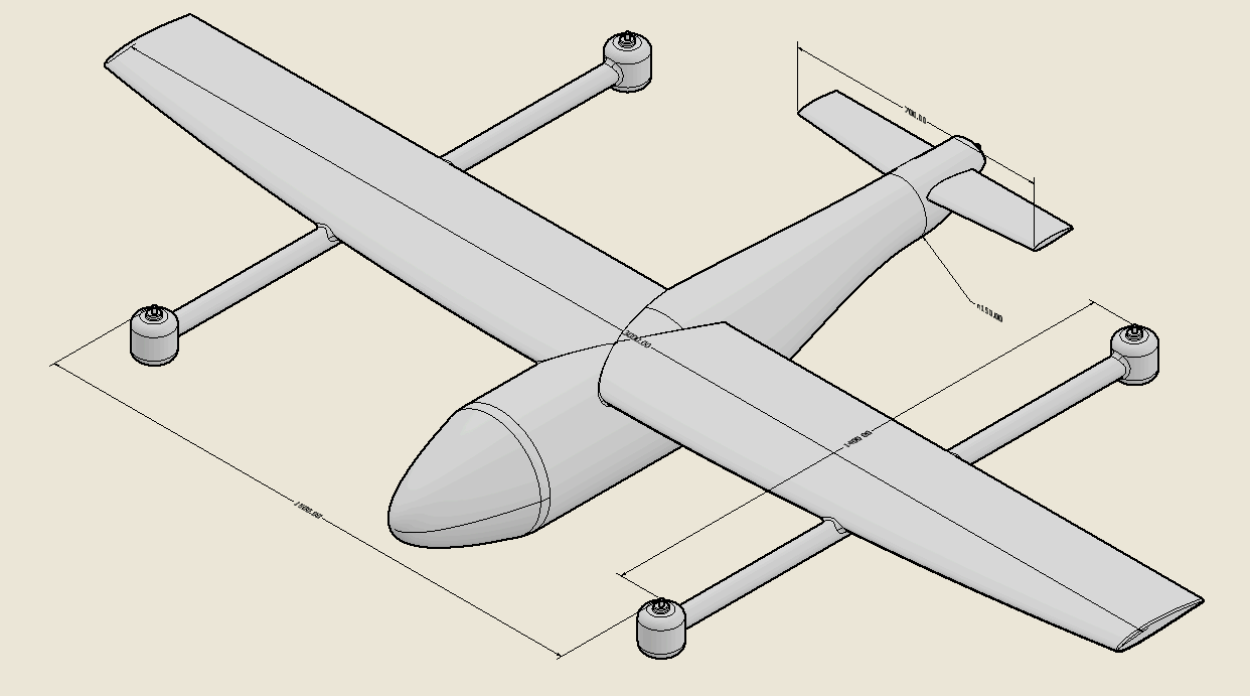

Figure 9. VTOL drone 3D design

The VTOL drone is far more complex than the previously discussed drones, having 3 main parts: the main body, wings, and propulsion system. The main body is made up of a series of cylindrical hulls of varying sizes, connected together into a smooth form to increase aerodynamic efficiency. It has a total length of 1.7 m and, at the widest, has a diameter of 30 cm. There are 2 sets of wings, each made of an airfoil to maximize lift. The main, larger wing has a total wingspan of 3 m, whereas the back

wings have a wingspan of 0.7 m. Finally, there are 5 propulsion systems on the drone, 4 on the wings and 1 on the back. The front propellers located on the wings allow the drone to fly vertically, whereas the back propellers are used in forward motion. Totally, the drone has a volume of 0.1169 m^3; assuming 4 mm thickness again, it weighs 2.574 kg.

Propulsion system:

The essential parts that allow drones to produce thrust and accomplish controlled flight are propulsion systems. Overall effectiveness, maneuverability, and mission suitability are all greatly impacted by the choice and performance of a propulsion system. Ion/plasma thrusters, photon thrusters, and propeller-based systems are the three main propulsion technology types that are the subject of this study, which all function according to different physical principles and are appropriate for various flight conditions. The use of each thruster type in the simulation, along with their specifications and outputs, will be covered in this section.

Propeller-based:

One of the most basic and common ways that aerial vehicles generate thrust is through propellers, particularly in drones and aircraft that operate in Earth's atmosphere. Through the aerodynamic interaction of the rotating blades with the surrounding air, they transform rotational motion from an engine or motor into linear thrust. By acting as airfoils, each blade generates a pressure differential that causes lift in the motion's direction, which moves the vehicle forward or upward. A propeller's diameter, blade pitch angle, number of blades, and rotational speed are among the design parameters that affect its efficiency and performance, affecting the amount of air acceleration and the propeller's ability to efficiently transform input power into useful thrust. Propellers also aid in stability and control in multirotor drones, and their varying speeds allow for three-dimensional maneuvering. Propellers, the most established and dependable propulsion system for atmospheric drones, are a key focus of this study in terms of efficiency and aerodynamic performance at various altitudes.

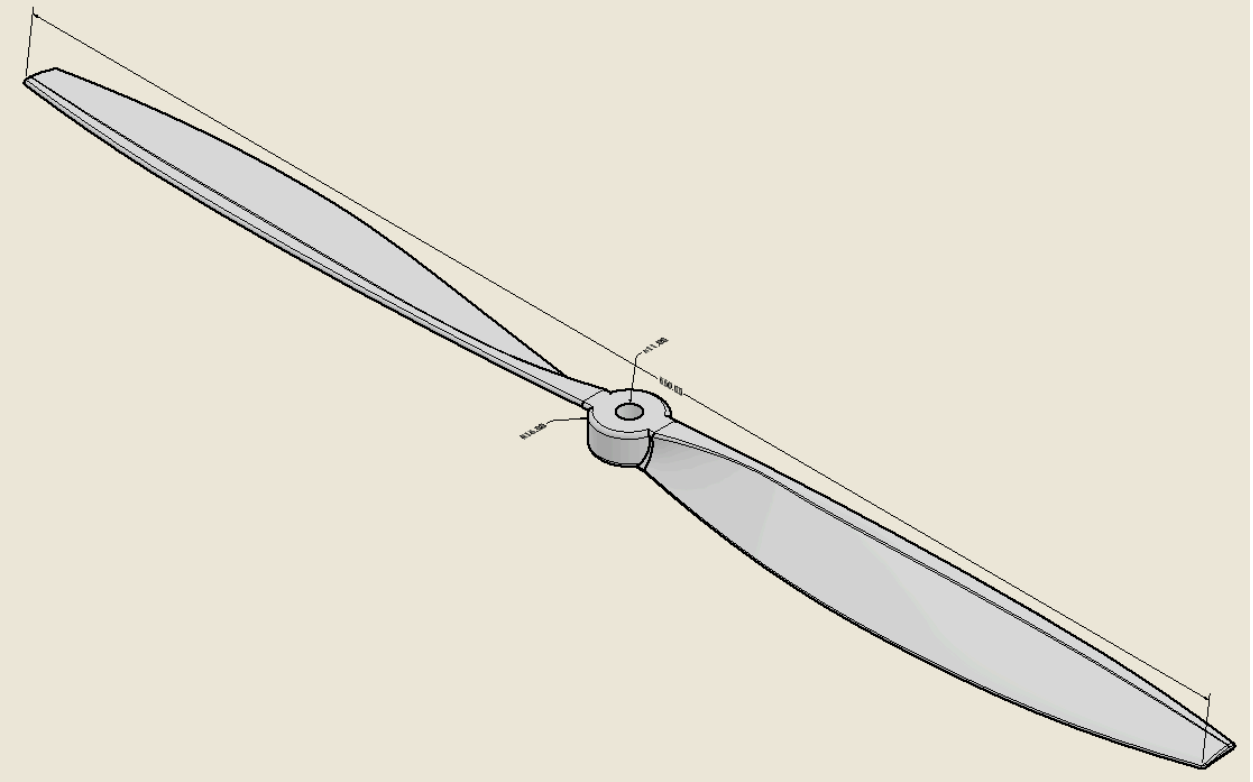

Figure 10. Propeller 3D design

The propellers have been meticulously modelled, paying close attention to the aerofoil characteristics to guarantee optimal performance in order to precisely replicate the lift produced by each drone. Each propeller has a maximum blade width of 4.5 cm at its widest point, a diameter of 66 cm, and a pitch of roughly 35.17 cm. In order to determine the overall thrust efficiency and aerodynamic behavior during flight simulations, these specifications are essential.

Given that larger drones typically operate between 2000 and 6000 RPM, or roughly 209 and 628 rad/s, we assume that the propeller must run at 500 rad/s; thus, the motor must be strong enough to maintain high-speed operation and lightweight enough to provide effective lift in order to reach this rotational speed. A brushless DC (BLDC) motor is chosen for this purpose because of its low weight, high efficiency, and dependability. These BLDC motors usually weigh between 150 and 600 grams, have a power rating of 300 to 1,000 watts, and have a voltage rating of 6 to 50 volts. We will assume that our motor, which weighs 300g and has a power rating of 500 W and a voltage rating of 24 V, falls somewhere in the middle of these ranges.

Ion thrusters:

Because of their high efficiency and ability to provide continuous thrust for extended periods of time, ion thrusters are a type of electric propulsion that has been extensively investigated for spacecraft and high-altitude applications. Ion thrusters work by ionizing a propellant (usually xenon) and using electric fields to accelerate the ions to extremely high velocities, expelling them at the back of the thruster. This is in contrast to conventional chemical propulsion systems, which rely on the combustion of fuel to generate a tiny but constant thrust. Ships propelled by this process can gradually reach high speeds over long stretches of time in a near-vacuum environment. Since they need a lot less propellant to get the same momentum as conventional chemical rockets, ion thrusters' main benefit is their exceptional fuel efficiency; therefore, they are perfect for long-duration or deep-space missions where mass conservation is essential. Since ion thrusters generate far less thrust than chemical rockets, they aren't well suited for launch or fast acceleration but can be utilized for fine control and fast travel in the vacuum of space. Their potential to offer effective propulsion in near-space environments where conventional propellers would be less effective due to the lower air density is the reason for the growing interest in their application for high-altitude drone technologies.

Due to the lack of commonly used ion thrusters in the necessary size and range, we will use operational models that are scaled down to approximate the weight. The NASA Solar Technology Application Readiness (NSTAR) (14) was a spacecraft that used ion thrusters as propulsion. The ship's thrusters weighed 8.3 kg and required 2.3 kW of power. Assuming that the power density stays the same, our thrusters with a power rating of 500 W would weigh approximately 1.46 kg. Using these values and the formula discussed in the literature review section, we can calculate the thrust produced.

$$T_i = I_b \sqrt{\frac{2m_i(U_b + U_p)}{q_0}} \quad (2)$$

T_i = Thrust (N)

I_b = Ion beam current (A)

m_i = Ion mass (kg)

U_b = Beam voltage (V)

U_p = Plasma potential (V)

q_0 = Elementary charge (C)

Assuming that the thrusters use xenon and the beam voltage reaches 1000V (typical range), we can find the beam current through the power and beam voltage $I_b = \frac{P}{U_b} = \frac{500W}{1000V} = 0.5A$. Now we have all the variables needed to solve the equation. Substituting all values, we get the answer, $T_i = 0.0264N$.

Photon thrusters:

Photon thrusters, also known as laser propulsion systems, represent one of the most innovative and futuristic methods of propulsion currently being explored for spacecraft and high-altitude applications. Unlike traditional propulsion systems that rely on the expulsion of mass (such as ion thrusters or chemical rockets), photon thrusters operate by emitting photons (light particles), which carry momentum. As photons are ejected at extremely high velocities from a laser or other light source, their momentum is transferred to the spacecraft, creating thrust. Although the force generated by photon thrusters is minuscule compared to other propulsion systems, their key advantage lies in their ability to provide continuous thrust without needing to ever refuel. This makes them highly efficient and ideal for long-duration missions, particularly in the vacuum of space, where the absence of atmospheric drag allows the propulsion system to operate unimpeded.

Photon laser thrusters are largely a theoretical system; thus, there is no current publicly accessible physical data from which we can draw assumptions. Therefore, we will also assume the thrusters have similar parameters to the ion thrusters, being a power rating of 500 W and a weight of 1.46 kg. This will provide us with a decent approximation of the actual values, which can be updated as more research is conducted. Using the values, we can compute the thrust using the formula of

$$F_t = (1 + r_1)\frac{W_{eq}}{c}$$

(3)

F_t is the total thrust generated (N)

W_{eq} is the laser power (W)

c is the speed of light (m/s)

r_1 is the reflectivity of the mirrors in the optical cavity.

Using a similar setup to the one discussed above, with reflectivity of 0.99999, we can compute the thrust, substituting all known values. Ultimately, the set-up is able to generate a thrust of $T_i = 3.3333 \times 10^{-6} N$ or $T_i = 3.3333 \mu N$.

Electrical Components:

A drone needs much more than just a structural frame and a propulsion system to operate efficiently, requiring numerous essential mechanical and electrical parts to make up a fully functional system. In order to operate continuously in high-altitude or space environments, these usually include a battery to power the motors and onboard systems, a central processing unit (CPU) to oversee control algorithms and decision-making procedures, a camera for visual monitoring and data collection, a transceiver to facilitate communication by sending and receiving signals, and a solar panel to recharge.

The exact choice, arrangement, and description of every single component, however, are outside the scope of this study; therefore, the characteristics and power requirements of all these subsystems will be referred to as a single, simplified "electrical pack," mostly based on the battery system's specifications, since the most important and heaviest part of a drone's electrical system is the battery pack. We can take into account the fundamental power and weight considerations related to drone operation by starting with the battery. Without unduly complicating the analysis, more components can be added to this model as needed to represent more intricate configurations. This method makes it possible to represent the drone's electrical architecture in a way that is both realistic and scalable.

Our drones, depending on the model, have 4-8 propellants, each requiring 500 W and 24 V, which the selected battery must be able to meet. To adequately supply the requirements in a lightweight form, the battery needs to have high discharge rates. For this purpose, Lithium Polymer (LiPo) is used for the high discharge, lightweight power delivery, and instant response, making it ideal for drones. When picking a power supply, two things are very important: to supply the required current, calculated through $I = \frac{P}{V}$ for each propellant, and to have adequate capacity. Assuming an average propulsion time of 10 min (a low-end estimate, however, still adequate for operation while in orbit), the batteries are chosen accordingly:

	Demanded Current	Demanded Capacity	Battery type	Capacity	Maximum Discharge	Mass
Quadcopter	83.333A	13.889 Ah	6 cell LiPo 25C	14Ah	350A	2.2 kg

Hexacopter	125A	20.833 Ah	6 cell LiPo 25C	21Ah	525A	3.1 kg
Octocopter	166.667A	27.778 Ah	6 cell LiPo 25C	28Ah	700A	4.1 kg
VTOL	104.167A	17.361 Ah	6 cell LiPo 25C	18Ah	450A	2.7 kg

Table 1. Battery specification

The batteries chosen have very high discharges, having more than double the requirement; they are more than adequate to supply the motors as well as any other electrical components, such as computing systems, measurement systems, visual systems, etc. Moreover, the batteries are relatively lightweight, weighing 2 - 4 kgs.

Introduction to ANSYS Fluent:

ANSYS Fluent is a computational fluid dynamics (CFD) software widely used in both academic and industrial research to simulate fluid flow, heat transfer, and other related physical phenomena. In the context of aerodynamic analysis, ANSYS Fluent provides a robust and flexible platform for simulating the complex interactions between air and the surfaces of flying vehicles, including unmanned aerial vehicles (UAVs) such as drones. Its ability to solve the Navier-Stokes equations with high accuracy makes it particularly suitable for analyzing airflow behavior, pressure distribution, lift and drag forces, and turbulence effects around aerodynamic bodies.

The software allows for both steady-state and transient simulations, enabling the study of various flight conditions and maneuvers. It supports advanced turbulence models such as k-ε, k-ω SST, and Large Eddy Simulation (LES), allowing for precise characterization of airflow. especially around multirotor configurations and complex geometries. In addition, Fluent's integration with ANSYS DesignModeler and meshing tools allows for seamless geometry import, preprocessing, and mesh refinement, which are crucial for capturing small-scale features that influence performance, such as rotor blade curvature or airframe structure.

For this study, ANSYS Fluent was chosen due to its proven reliability, accuracy, and versatility in modelling aerodynamic phenomena across a wide range of applications. Its use enables the investigation of critical parameters such as pressure distribution, velocity fields, wake regions, and vortex formation around drone structures. By using Fluent’s post-processing capabilities, the resulting data can be visualized and analyzed in depth, facilitating design optimization and comparative evaluation of different drone and propulsion configurations. Thus, ANSYS Fluent serves as an essential tool in developing a comprehensive understanding of drone aerodynamics under realistic operational conditions.

Assumptions:

Throughout the course of this study, a number of assumptions have been made to streamline the modelling and simulation process. These assumptions pertain to both component-specific parameters and broader environmental and simulation conditions. In this context, assumptions serve two main purposes. First, they provide a basis for selecting fixed values for certain parameters where variability is either minimal or beyond the scope of the study, such as the battery capacity, material properties, or atmospheric composition. Second, they define the boundary and initial conditions necessary for computational simulations, including constant pressure and temperature, gravitational force at specific altitudes, and the initial velocities or positions of the drones. This section will outline all such assumptions, providing clarity on the basis of the models and simulations used.

Physical assumptions:

Overall, the primary purpose of the physical assumptions in this study has been to establish a reasonably accurate mass model of each drone configuration. Since many critical performance parameters, most notably gravitational force, are directly influenced by the drone's mass, it is essential to have a consistent and realistic estimation of weight. By approximating the total weight through careful consideration of key components such as the frame, propulsion system, and especially the battery, calculation of acting forces can be done with precision.

When selecting the components for modelling and simulation in this study, we deliberately chose mid-range parameter values. This approach was taken to ensure a balanced and unbiased representation of performance, avoiding the extremes of either overly optimistic, high-end specifications or overly conservative, low-end limitations. By selecting components that reflect commonly available, moderately capable technology, the analysis remains grounded in realistic engineering conditions.

This consideration directly informs the selection and definition of several key parameters in our study, including the drone's frame, affecting not only the structural integrity and stability of the drone but also influencing the placement of propellers and the distribution of lift; the specifications of the electrical components, particularly the battery pack making up a major part of the weight; and the characteristics of the propulsion systems, each having unique performance characteristics and mass requirements. Each of the components is displayed in the table below.

Propeller	Volume (mm^3)	Frame mass	Propulsion	Electrical pack	Total

Quadcopter	106004337.7 mm³	2.3334 kg	1.2 kg	2.2 kg	5.7334 kg
Hexacopter	111988344.6 mm³	2.4651 kg	1.8 kg	3.1 kg	7.3651 kg
Octocopter	117972348.3 mm³	2.5968 kg	2.4 kg	4.1 kg	9.0968 kg
VTOL	116931917 mm³	2.5739 kg	1.5 kg	2.7 kg	6.7739 kg

Table 2. Propeller-based drone weight

Ion	Volume	Frame mass	Propulsion	Electrical pack	Total
Quadcopter	106004337.7 mm³	2.3334 kg	5.8571 kg	2.2 kg	10.3905 kg
Hexacopter	111988344.6 mm³	2.4651 kg	8.7857 kg	3.1 kg	14.3508 kg
Octocopter	117972348.3 mm³	2.5968 kg	11.7142 kg	4.1 kg	18.4111 kg
VTOL	116931917 mm³	2.5739 kg	7.3214 kg	2.7 kg	12.5953 kg

Table 3. Ion-based drone weight

Photon	Volume	Frame mass	Propulsion	Electrical pack	Total
Quadcopter	106004337.7 mm³	2.3334 kg	5.8571 kg	2.2 kg	10.3905 kg
Hexacopter	111988344.6 mm³	2.4651 kg	8.7857 kg	3.1 kg	14.3508 kg
Octocopter	117972348.3 mm³	2.5968 kg	11.7142 kg	4.1 kg	18.4111 kg
VTOL	116931917 mm³	2.5739 kg	7.3214 kg	2.7 kg	12.5953 kg

Table 4. Photon-based drone weight

Initializing assumptions:

The purpose of these assumptions is to establish a clear and consistent set of initial conditions that ensure the simulation remains both unbiased and reproducible. By standardizing certain environmental and operational parameters, we can effectively isolate the aerodynamic behavior of each drone configuration and accurately compare their performance across various propulsion methods.

To model the airflow around the drone accurately, we utilized the transient k-epsilon (k-ε) turbulence model in ANSYS Fluent. This model is widely used in computational fluid dynamics (CFD) for simulating turbulent flows. It offers a good balance between computational efficiency and accuracy, making it particularly suitable for external aerodynamic simulations involving drones. The k-epsilon model accounts for turbulent kinetic energy (k) and its dissipation rate (ε), which allows it to effectively predict complex flow patterns such as vortices and wake regions around the drone's structure. The transient aspect of the model enables us to capture time-dependent fluctuations in the airflow, which are crucial for understanding dynamic aerodynamic forces like unsteady lift and drag that occur during real flight.

In terms of drone operation, drones of the size and class considered in this study typically feature propeller speeds ranging from 4,000 to 10,000 revolutions per minute (RPM). For the sake of consistency and simplicity, we assume each propeller operates at a steady angular velocity of 500 rad/s, which corresponds approximately to 4,774 RPM. This value represents a mid-range operational speed for high-performance multirotor drones and ensures that the thrust generation remains stable throughout the simulation.

Additionally, to evaluate the aerodynamic drag under realistic flight conditions, we assume that each drone is flying at a constant forward velocity of 20 meters per second. This speed is representative of performance-capable drones used in surveillance, mapping, and high-altitude applications. By fixing this flight velocity, we can perform consistent drag analysis across all drone types and propulsion configurations.

These assumptions collectively form the foundation of our simulation environment, allowing for a fair and controlled comparison of each drone's aerodynamic behavior under equivalent conditions. These values are not meant to represent the absolute limits or capabilities of any single drone but rather to provide a consistent baseline that reflects realistic operational scenarios. By doing so, we can establish meaningful trends and comparisons between different drone configurations and propulsion systems. This approach enables us to obtain reliable estimates of aerodynamic performance, thrust generation, and drag forces, even in the absence of fully detailed, real-world flight data for every design considered.

Chapter 4: Results and Discussion

This section presents a comprehensive analysis of the data gathered through an extensive series of simulations conducted using ANSYS Fluent. A total of 172 simulations were performed, each comprising 100 iterations, to ensure convergence and accuracy. These simulations spanned four primary drone categories: quadcopter, hexacopter, octocopter, and VTOL. This thorough approach allows for a detailed and fair comparison of the drones' performance under controlled environments.

We begin by presenting the simulation results for each drone type. For every drone, key performance metrics are analyzed under identical conditions to ensure a fair and consistent comparison. These simulations were conducted under standard atmospheric conditions at sea level, with the assumption that each drone is flying at a steady velocity of 20 meters per second during the drag analyses. The evaluated

parameters include multi-directional drag, lift and thrust generation, and overall flow behavior, each of which helps to characterize the aerodynamic profile and efficiency of the drones across various flight scenarios.

The simulation results are plotted into comparative graphs and summary data visualizations. These allow for an integrated view of how each drone performs relative to the others. Trends are identified and discussed, highlighting specific strengths and limitations of each design. This analysis ultimately aids in evaluating which drone types are most suited for particular use cases based on their aerodynamic performance and propulsion efficiency.

Finally, the synthesized data will be utilized to determine the **effective operational range** of all three propulsion types: **propeller-based**, **ion**, and **photon thrusters**. By integrating aerodynamic performance results with parameters of **mass** and **thrust output**, the study aims to estimate how far each propulsion method can effectively carry its respective drone configuration under realistic conditions. This evaluation will provide crucial insight into the practical applicability of each propellant system. particularly in terms of **altitude capability** and **suitability for space or near-space operations**.

Data of individual drones:

This section examines how the structural design of each drone type influences key aerodynamic parameters such as lift, drag, and stability. By analyzing these effects individually, we gain a deeper understanding of how specific design choices, such as rotor configuration, body shape, and weight distribution, impact overall performance. The example simulations presented here are all conducted under standard atmospheric conditions at sea level to ensure consistency and eliminate altitude-based variability. This provides a clear baseline for comparison across the different drone models before evaluating performance in more complex or high-altitude environments.

Quadcopter:

The quadcopter represents the most fundamental and widely used configuration among the drones analyzed in this study. Due to its relatively simple structure, featuring four motors arranged symmetrically, it serves as a baseline model against which the performance of more complex drone types can be effectively compared. Its limited number of rotors generally results in lower overall thrust capacity compared to drones with more motors, which may restrict payload capabilities and reduce performance under high-load conditions. However, the compact and symmetrical design of the

quadcopter offers aerodynamic advantages. The smaller frame reduces the overall surface area exposed to airflow, thereby minimizing drag.

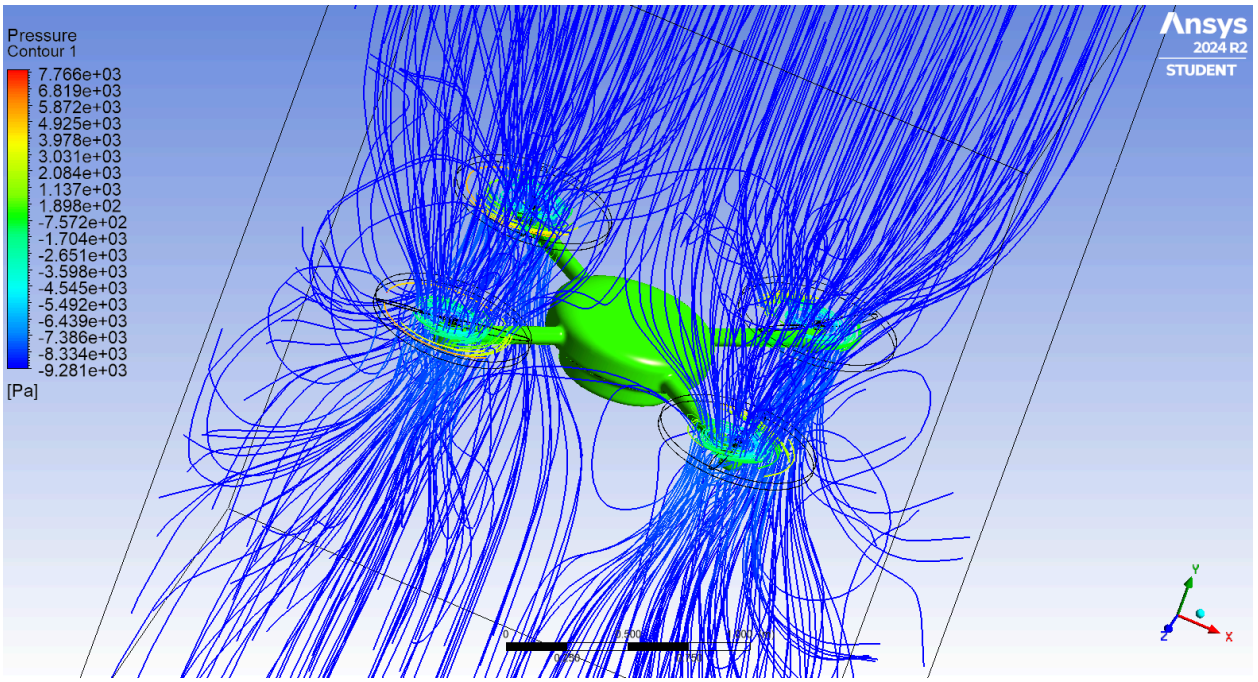

Figure 11. Quadcopter lift simulation

The figure illustrates the simulation results for calculating the thrust generated by the propellers. To isolate the pure thrust force, the simulation was conducted by eliminating all external influences such as gravitational forces and wind currents acting on the drone. This approach ensured that only the propeller-induced forces were captured. As seen in the figure, the simulation accurately reflects the expected behavior of airflow around the drone. The blue streamlines represent the velocity of air currents, showing air starting at lower speeds and then accelerating as it is drawn in and expelled by the spinning propellers. This movement generates upward thrust at each propeller. Additionally, as the accelerated air is pushed downward, it exerts a reactive force on the drone's frame, contributing further to the total thrust produced. In this specific simulation, the total thrust force, considering both body drag and the force of the four propellers, is approximately 131.27 N.

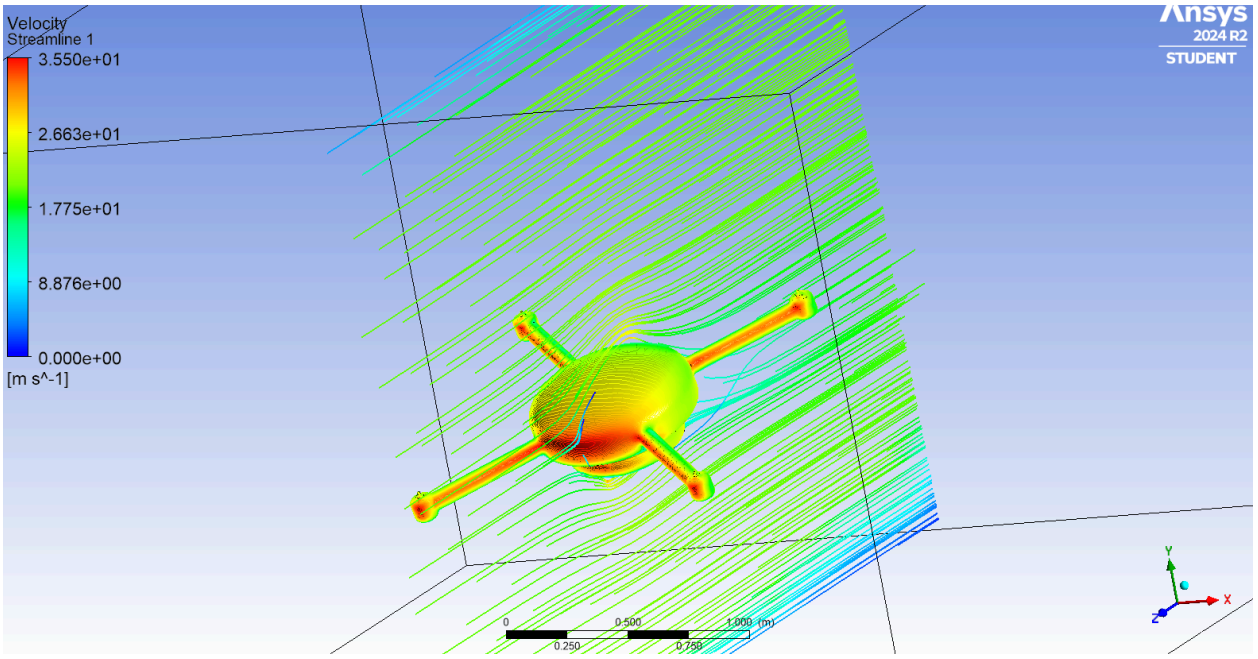

Figure 12. Quadcopter horizontal drag simulation

The figure above shows the simulation results for calculating the drag experienced by the drone during horizontal motion. As discussed earlier in the literature review, the drone is tilted at a 20-degree angle, which is a typical flight configuration for drones during horizontal flight. This tilt increases the drag compared to a level flight posture, as the air resistance becomes higher at the tilted angle. However, the impact of drag can be mitigated with a more streamlined or aerodynamic design, which helps reduce the resistance encountered by the drone. In this simulation, the drone experiences a drag force of approximately 28.67 N.

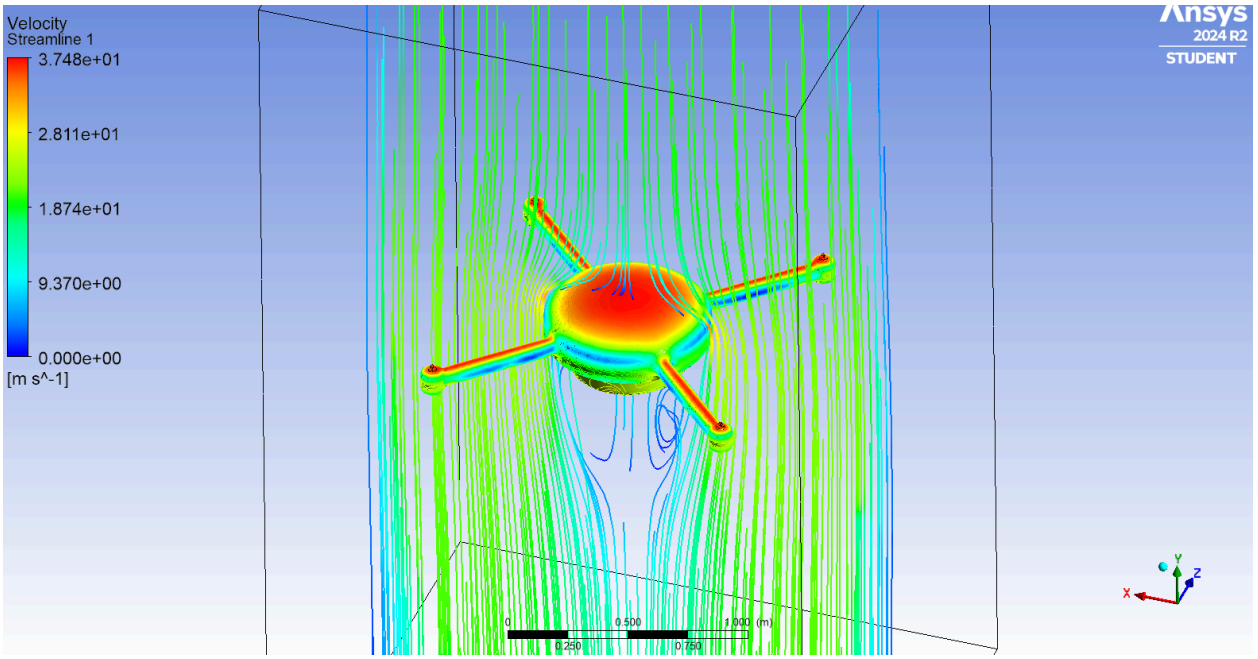

Figure 13. Quadcopter vertical drag simulation

Due to the increased surface area exposed to the direction of motion, vertical motion in drones is one of the most energy-intensive actions, requiring overcoming greater drag forces compared to horizontal flight. Depending on the design, this effect can be reduced or greatly increased. As shown in the illustration, our drone, despite having a domed exterior, is also less aerodynamic when moving vertically. The drone experiences a drag force of approximately 68.28 N, which is more than double the drag encountered during horizontal motion.

Hexacopter:

The hexacopter represents a more advanced configuration compared to the quadcopter, with six motors arranged symmetrically. This design provides a significant increase in thrust capacity, allowing for better payload capabilities and enhanced performance, particularly in high-load or demanding conditions. The additional motors not only improve thrust but also contribute to greater stability and redundancy, reducing the risk of total failure in case one motor malfunctions. However, the larger frame size compared to the quadcopter results in an increase in the overall surface area exposed to airflow, which leads to a higher drag and increased weight.

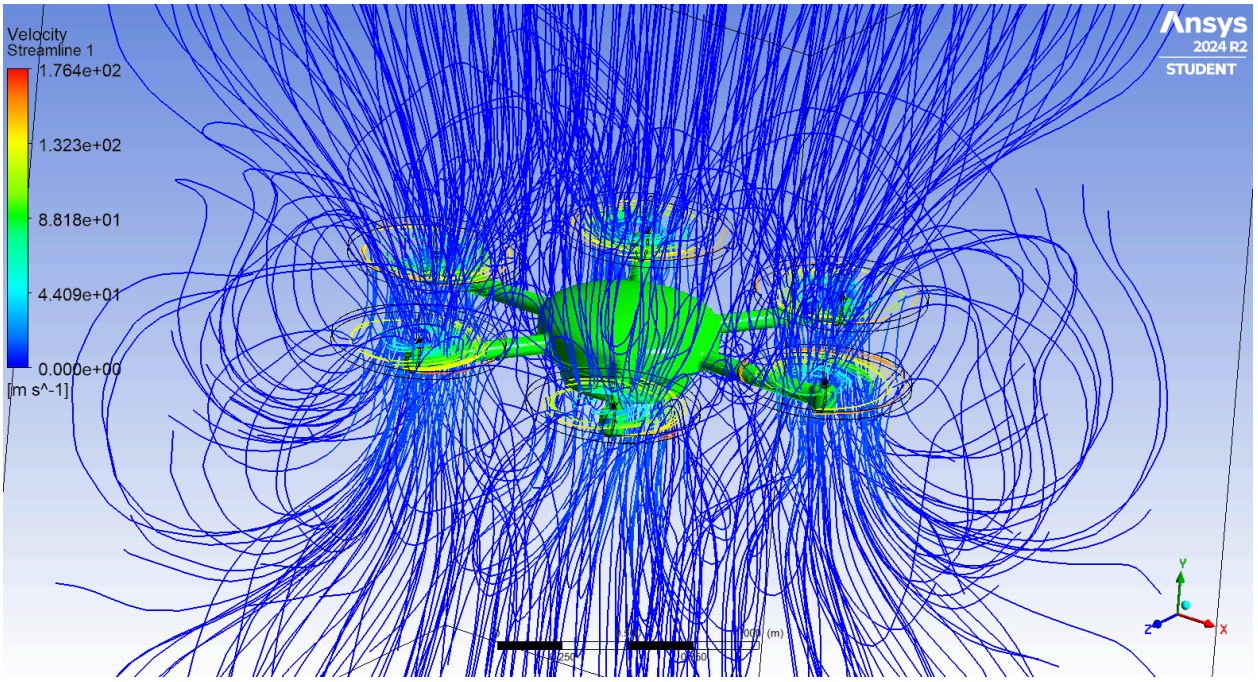

Figure 14. Hexacopter lift simulation

The figure above displays the thrust simulation results for the hexacopter. Compared to the previous simulation, the air currents around the hexacopter are noticeably more turbulent and chaotic. Despite having six motors, the drone generates a thrust of 174.41 N, which is significantly less than expected when compared to the

thrust force of a quadcopter with just four motors. This observation indicates that the relationship between the number of motors and the resulting thrust is not linear. Adding more motors does not necessarily result in a proportional increase in thrust, suggesting that other factors, such as aerodynamic interactions and design considerations, play a crucial role in determining overall thrust generation.

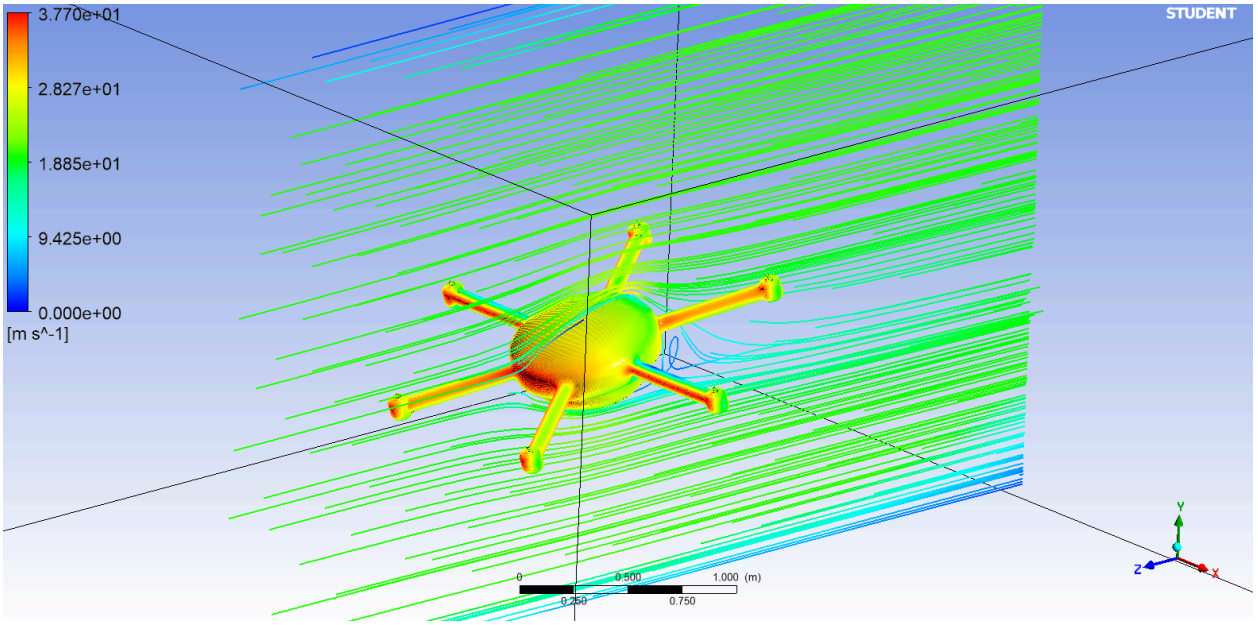

Figure 15. Hexacopter horizontal drag simulation

The hexacopter, with its additional arms and different structural configuration, experiences significantly greater horizontal drag, as clearly demonstrated by the simulation results. It encounters a total drag force of 42 N, representing an approximate 46.5% increase compared to the quadcopter. This highlights that in aerodynamic design, not only the total surface area but also the arrangement and orientation of structural components play a critical role in influencing and minimizing parasitic drag. The added complexity and broader layout of the hexacopter contribute to higher resistance during forward motion, emphasizing the importance of compact and streamlined designs for improved aerodynamic performance.

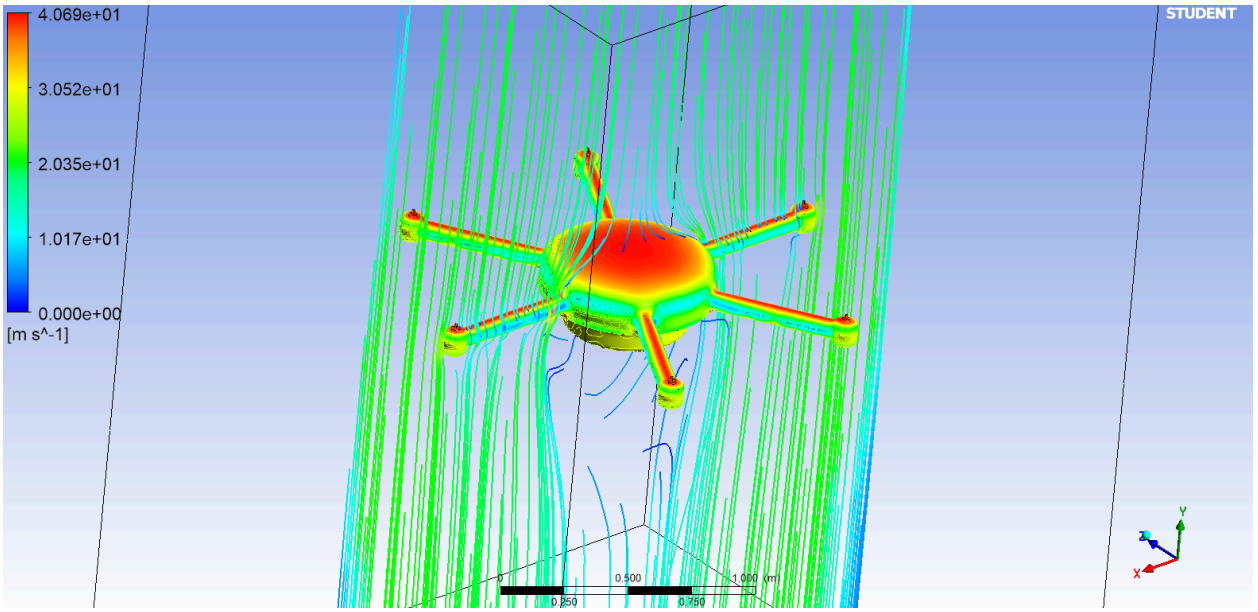

Figure 16. Hexacopter vertical drag simulation

The figure above presents the simulation results illustrating the effects of horizontal flight on the hexacopter. Due to the increased surface area from its additional arms, the hexacopter experiences higher drag compared to the quadcopter. Similar to the behavior observed in the quadcopter, the hexacopter is subjected to significantly greater drag during vertical motion than during horizontal flight. Specifically, it experiences approximately 83.44 N of vertical drag compared to 42 N of horizontal drag, nearly double the resistance.

Octocopter:

The octocopter represents the most powerful and advanced configuration among the drones analyzed in this study. With eight motors arranged symmetrically, it provides significantly greater thrust capacity compared to the quadcopter and hexacopter, allowing it to carry heavier payloads and maintain better performance under demanding conditions. However, this increase in motor count and structural complexity also introduces notable aerodynamic challenges. The larger frame and additional arms increase the overall surface area exposed to airflow, thereby elevating drag as well as increasing weight.

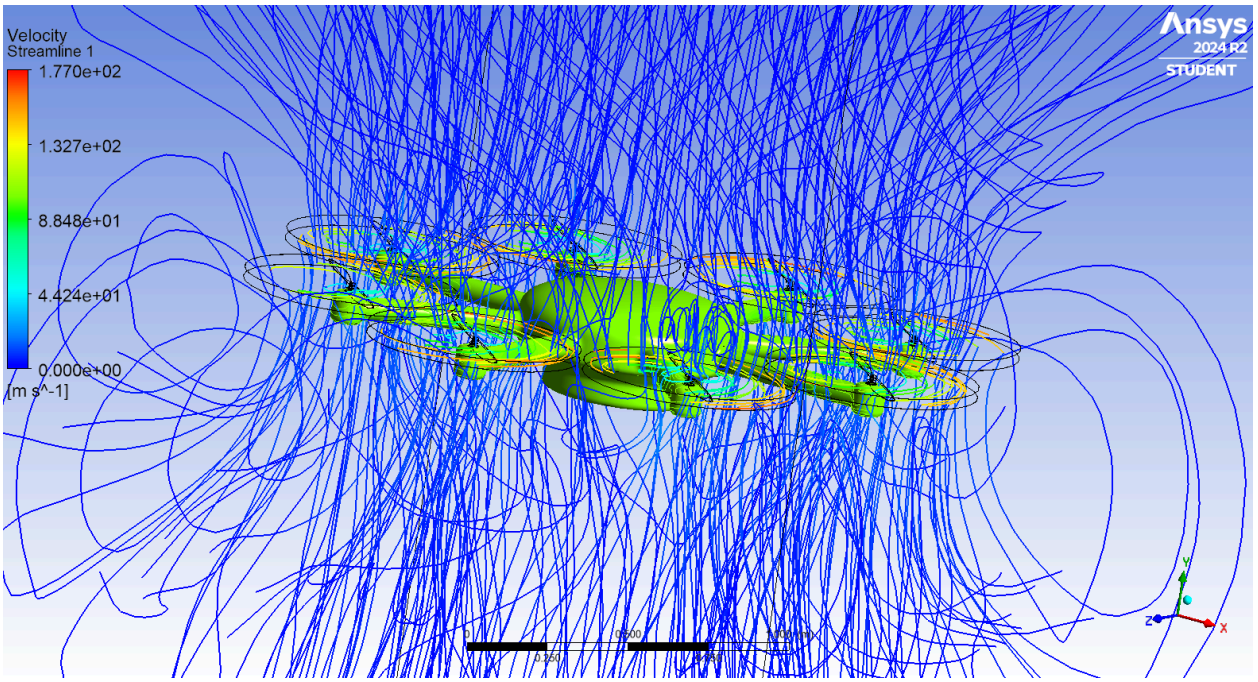

Figure 17. Octocopter lift simulation

The simulation results clearly show that the airflow generated by the octocopter's propellers is highly chaotic, with noticeable vortices forming and interfering with one another. This turbulence is likely due to the close proximity of the propellers, causing them to draw air from each other and disrupt normal airflow patterns. As a result, the efficiency of each propeller is significantly reduced. Instead of the expected 260 N of total thrust, based on scaling from the quadcopter's performance, the octocopter produces only 207.4 N. This highlights a crucial design consideration of ensuring sufficient spacing between propellers to maintain optimal aerodynamic efficiency and avoid detrimental interference effects.

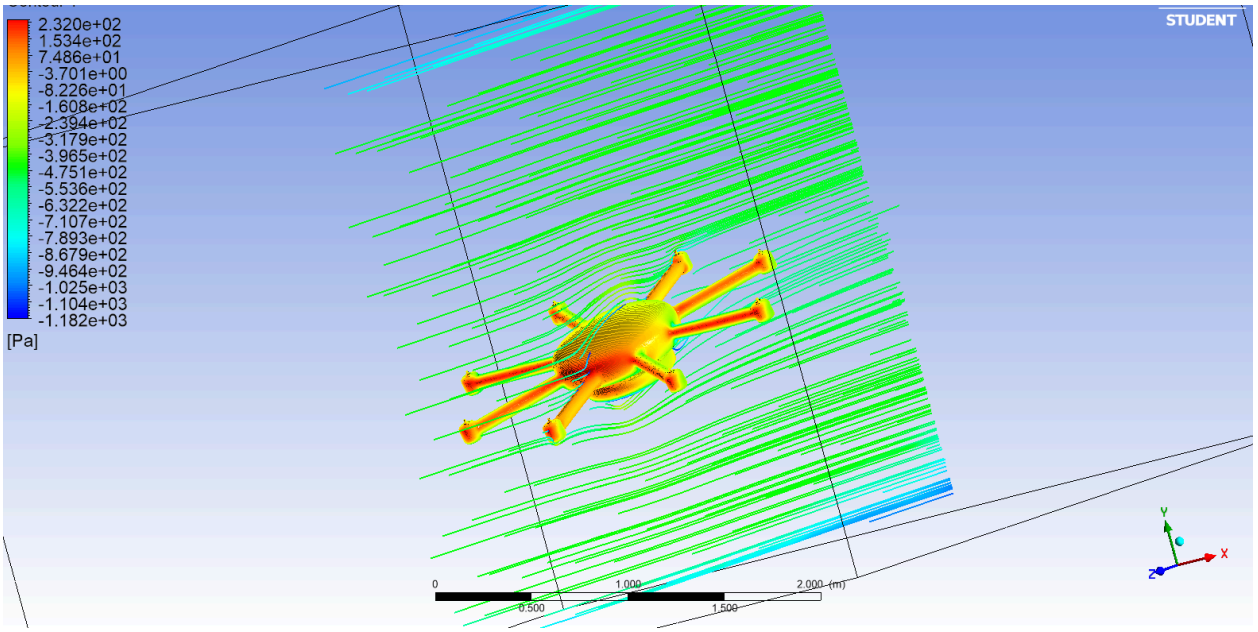

Figure 18. Octocopter horizontal drag simulation

The figure above shows the simulation results of the octocopter in horizontal motion, revealing a total drag force of 37.29 N. Interestingly, despite the octocopter having more surface area due to its additional arms, it experiences less horizontal drag than the hexacopter, which recorded a drag of 42 N. This indicates that the octocopter's more compact and symmetric configuration helps to disrupt vortex formation and streamline airflow around the body, resulting in improved aerodynamic performance. These results emphasize that, in drone design, the overall configuration and shape play a more critical role in reducing drag than surface area alone.

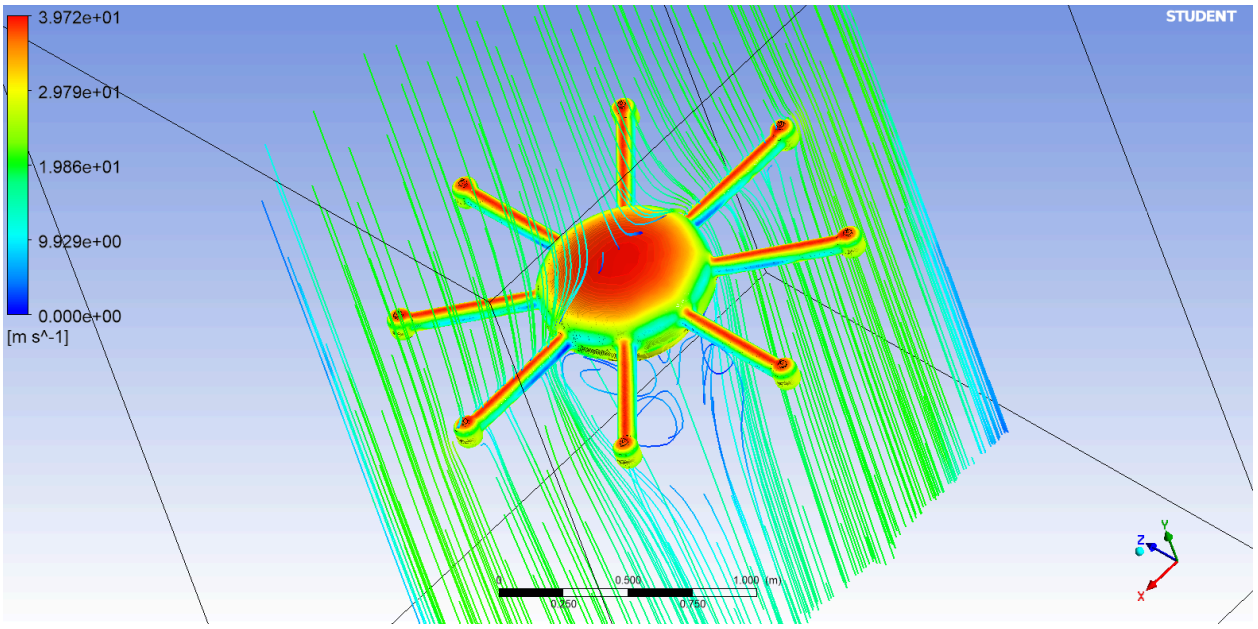

Figure 19. Octocopter vertical drag simulation

Similar to the results of the quadcopter and hexacopter, the vertical drag of the octocopter shows a proportional increase with regards to the exposed surface area in the direction of motion. The simulation shows a total vertical drag of 96.59 N for the octocopter, which is approximately a 41.44% increase from the quadcopter and a 14.76% increase from the hexacopter.

VTOL drone:

The VTOL drone represents a more complex configuration compared to the multicopter designs analyzed in this study. Unlike traditional multicopters that rely solely on multiple propellers for lift and movement, VTOL drones integrate fixed wings along with vertical lift systems, enabling efficient flight in both vertical and horizontal modes. This dual capability allows VTOLs to achieve greater range and endurance. The streamlined design of the wings significantly reduces drag during horizontal cruising; however, the added wings and control surfaces change the aerodynamic properties, causing increased drag during vertical flight. Despite these trade-offs, VTOLs are highly effective for long-distance and high-efficiency missions. As such, the VTOL configuration provides an important point of comparison against purely rotor-based drones.

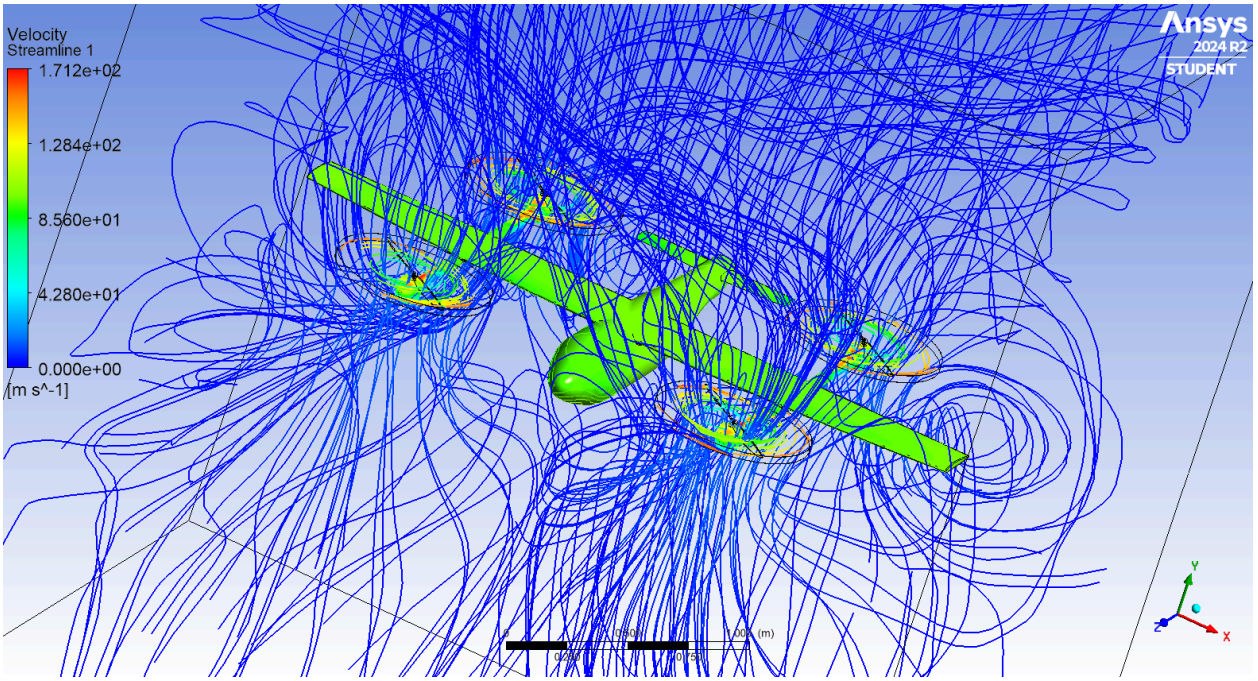

Figure 20. VTOL lift simulation

The VTOL drone is equipped with a total of five rotors, four dedicated to vertical flight and one for horizontal propulsion. The figure above illustrates the simulation results for vertical thrust generation using the four vertical rotors. It is evident from the figure above that since the rotors are positioned farther apart compared to those on a

quadcopter, each rotor has access to a larger volume of undisturbed air. As a result, despite having the same number and type of motors and propellers as the quadcopter, the VTOL drone generates slightly more thrust, reaching 139.85 N. This highlights the critical role of rotor spacing in optimizing airflow and maximizing thrust efficiency, emphasizing that proper spatial arrangement of propellers is crucial for proper airflow.

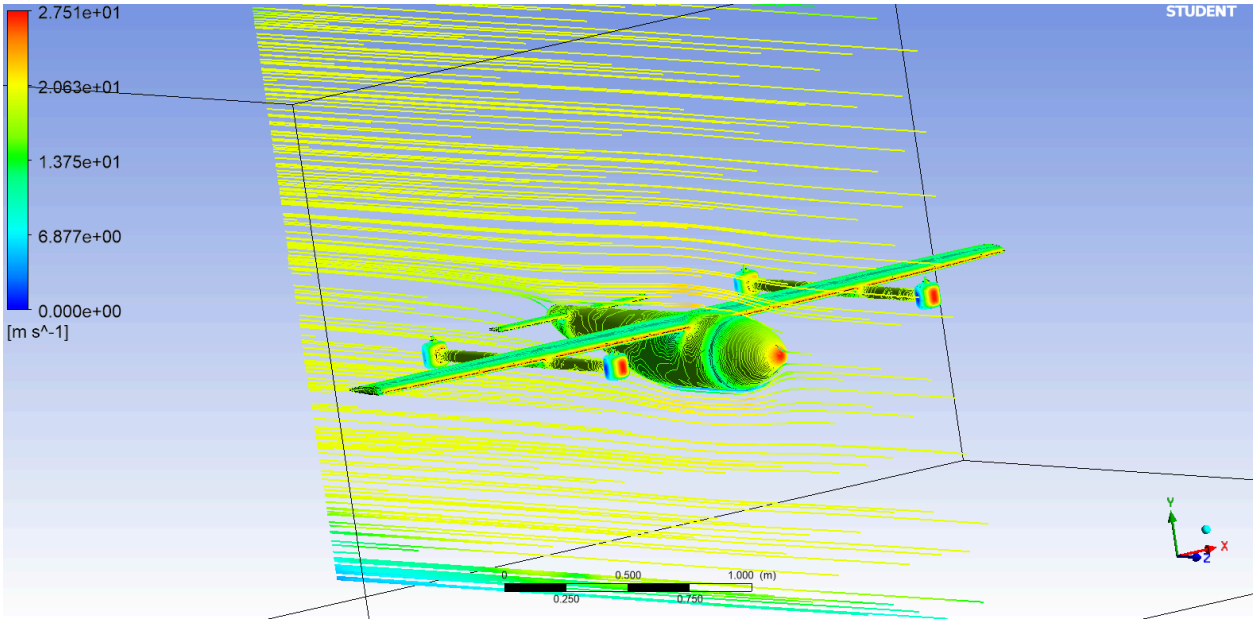

Figure 21. VTOL horizontal drag simulation

The primary advantage of the VTOL drone lies in its exceptional efficiency during horizontal flight. Specifically engineered for long-distance travel, its streamlined geometry effectively manages and distributes airflow, significantly minimizing drag. The simulation results reveal that the VTOL drone experiences a total horizontal drag of just 10.72, despite being one of the larger drones examined in this study. This value is the lowest recorded drag among all drone types analyzed, clearly establishing the VTOL as the most aerodynamically efficient option for sustained horizontal motion.

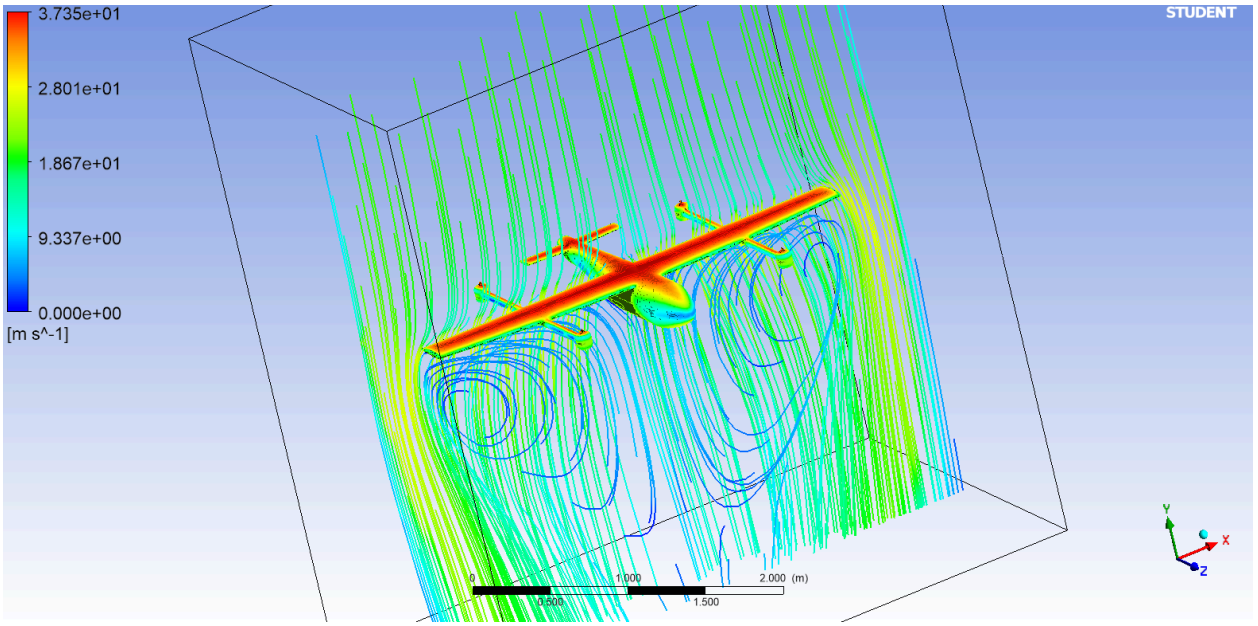

Figure 22. VTOL vertical drag simulation

On the other hand, VTOL drones are extremely inefficient during vertical motion, performing worse than all the other drone types analyzed. The very design features that enhance their efficiency in horizontal flight, such as large wings acting as aerofoils and an elongated body structure, become significant disadvantages when flying vertically, dramatically increasing drag. The simulation results show that the vertical drag acting on the VTOL drone is approximately 500.14 N, more than five times greater than the drag experienced by the other drones. This highlights the critical importance of clearly defining the intended purpose of a drone during the design phase, as design elements that offer advantages in one flight regime can become major drawbacks in another.

Comparison plots:

This section will present the results of the study concerning how the key performance parameters of each drone design evolve across varying altitudes. By systematically plotting the data, we will visualize the trends in factors such as thrust generation, drag forces, and overall aerodynamic efficiency. This comparative analysis will allow us to better understand how altitude affects the performance of each drone type. Ultimately, these results will be synthesized to evaluate and rank the overall effectiveness of each design, helping to determine which configuration offers the best performance under changing atmospheric conditions.

Lift/Thrust:

Thrust is one of the most critical parameters in drone performance, as it determines both the carrying capacity and whether the drone can achieve and sustain flight at all. The plot below illustrates how the generated thrust varies for each drone type as a function of altitude. By analyzing these trends, we can better understand the operational limits and effectiveness of each design in different atmospheric conditions.

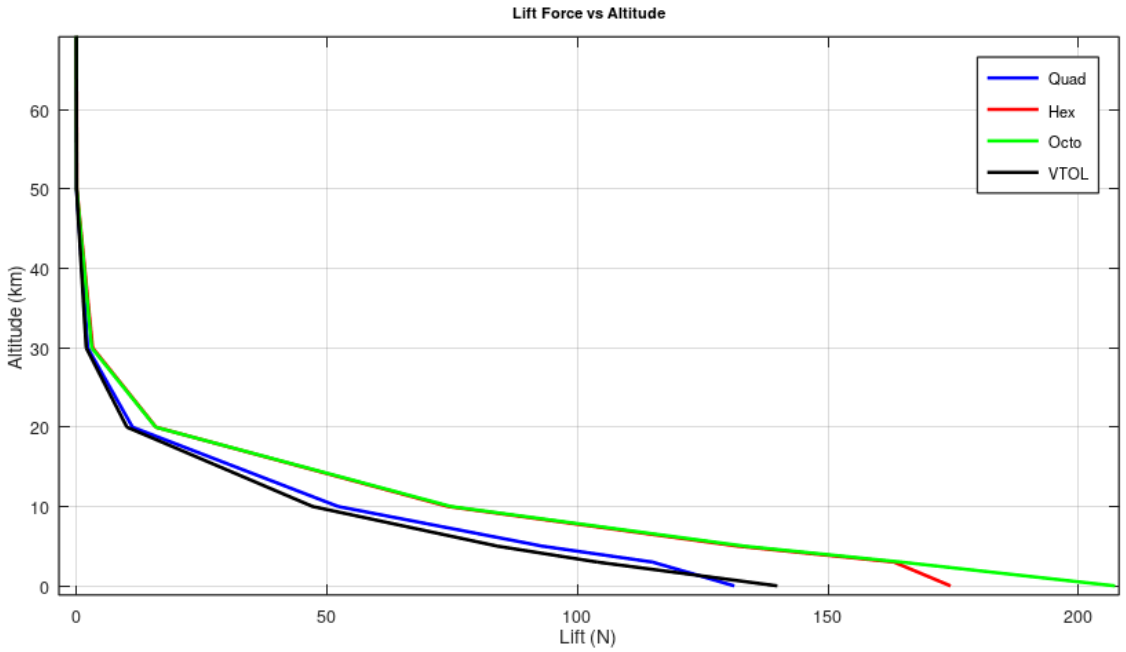

Figure 23. Lift vs altitude plot

The graph shows that the quadcopter and VTOL drones generate nearly the same amount of thrust across the range of altitudes studied. This outcome is expected, given that both drones are equipped with the same number of rotors, four in total. Initially, the VTOL drone produces slightly more lift, but the quadcopter quickly overtakes it as altitude increases. However, the difference between the two remains minimal, indicating that their thrust capabilities are largely comparable under similar conditions.

What is more surprising is the relationship between the hexacopter and the octocopter. Initially, both drones perform as expected, with the octocopter generating significantly more thrust than the hexacopter and both producing far greater thrust than the quadcopter and VTOL drones. However, this trend quickly shifts as altitude increases. with the thrust outputs of the hexacopter and octocopter gradually converging to nearly identical values. This behavior can likely be attributed to the increased turbulence and vortex interference in the octocopter, as discussed in previous sections. As altitude rises and air density decreases, the chaotic airflow around the closely spaced propellers of the octocopter becomes even more

pronounced, leading to a rapid decline in its efficiency. Ultimately, the octocopter's performance drops to match that of the hexacopter. This result suggests that, within the parameters and conditions set by this study, the hexacopter represents the most efficient design, maintaining its performance advantage more consistently across altitudes.

Finally, since thrust is entirely dependent on air density, it decreases sharply with increasing altitude. Because air density drops exponentially with height, the thrust also diminishes rapidly at first, then gradually slows its decline as it approaches zero. From the graph, we can observe that thrust becomes essentially negligible around 50 kilometers in altitude. This point represents the theoretical upper limit for propeller-based drones. Beyond this altitude, even a massless drone would be unable to generate sufficient lift to sustain flight. Thus, this finding highlights a fundamental limitation of propeller-driven systems in high-altitude applications.

Horizontal drag:

When conducting long-distance missions, maximizing efficiency becomes critically important. One of the key factors influencing this efficiency is horizontal drag, which largely determines how much energy the drone must expend to maintain forward motion. The plot below illustrates how horizontal drag varies with altitude. By analyzing these trends, we can better understand how different designs perform and identify the characteristics needed to develop more aerodynamically efficient drones optimized for sustained horizontal flight.

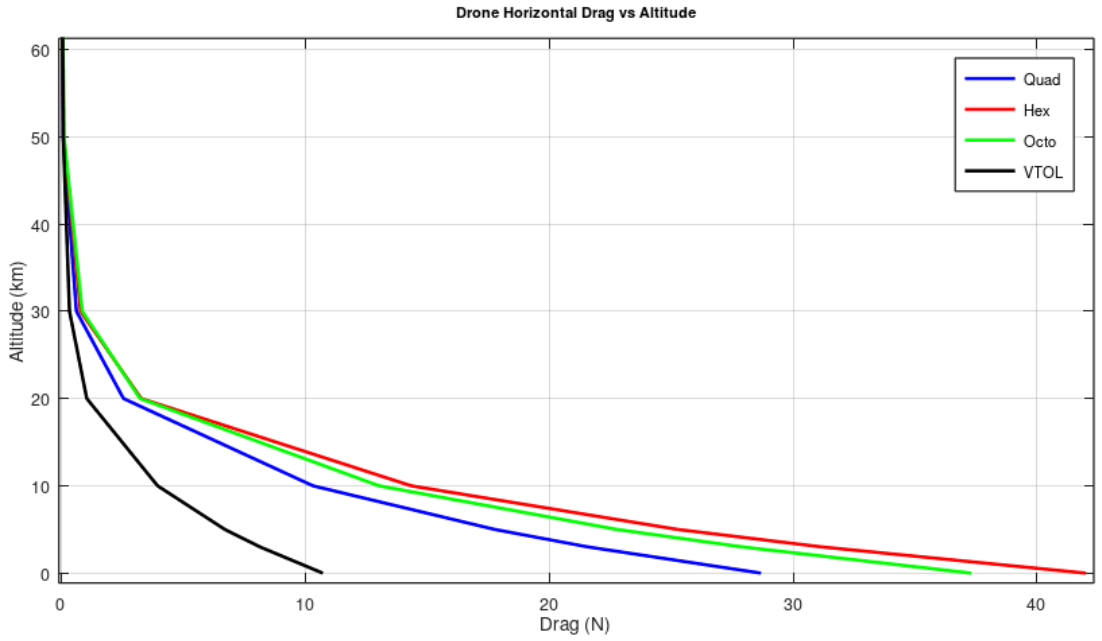

Figure 24. Horizontal drag vs altitude plot

From the graph, it is clear that the VTOL drone is by far the most efficient design for horizontal motion, experiencing nearly three times less drag than any of the other configurations. Its reduced frontal surface area and streamlined aerodynamic shape significantly improve airflow around the body, minimizing vortex formation and overall drag across all altitudes. This demonstrates that, even when a drone has a larger overall surface area, thoughtful aerodynamic design can dramatically enhance its efficiency, especially during horizontal flight.

In the previous section, we observed that despite having a larger overall surface area, the octocopter experienced less horizontal drag than the hexacopter. The graph further confirms that this behavior was not a one-time occurrence; across all altitudes, the octocopter consistently experiences lower drag than the hexacopter. This finding reinforces the idea that the overall configuration and arrangement of parts play a critical role in aerodynamic performance, often outweighing the simple consideration of surface area alone.

Similar to the behavior observed in the thrust graph, the horizontal drag also decreases exponentially with altitude due to its dependence on air density, becoming negligible for all drone designs around 50 kilometers. This suggests that at higher altitudes, aerodynamic design becomes largely irrelevant, provided a sufficiently powerful propulsion method is employed. However, it is important to note that while the drag becomes very small, it never truly reaches zero. This residual drag, although minor, becomes increasingly significant in the next section, where even very small forces generated by alternative thrusters must be carefully considered.

Vertical drag:

When conducting missions that require frequent or sustained climbs to higher altitudes, maximizing efficiency in vertical motion becomes critically important. Vertical drag is the most important parameter in such scenarios, as it largely determines how much energy the drone must expend to ascend. The plot below illustrates how vertical drag varies with altitude. By analyzing these trends, we can gain insights into how different drone designs perform during vertical flight and identify the key characteristics necessary to create more aerodynamically efficient drones optimized for climbing and high-altitude operations.

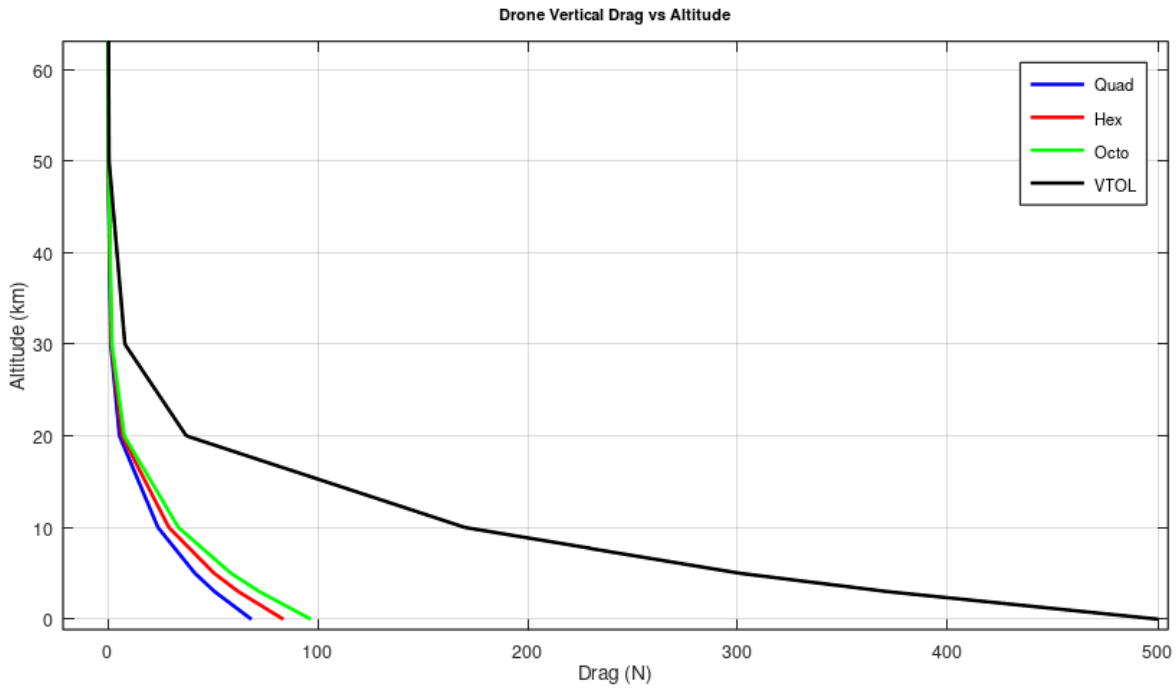

Figure 25. Vertical drag vs altitude

The most striking feature of the graph is how clearly it highlights the inefficiency of VTOL drones in vertical motion compared to other designs. Across all altitudes, VTOL drones experience nearly five times more vertical drag than the other drone types. This inefficiency stems from a significant design trade-off: the features that greatly enhance the VTOL's performance in horizontal motion become major liabilities during vertical ascent. This result strongly reinforces the principle that the intended mission profile of a drone must be carefully defined before finalizing its design, as design advantages in one area can easily become critical disadvantages in another.

In contrast, the simpler designs of the octocopter, hexacopter, and quadcopter demonstrate a more predictable and proportional relationship between surface area and vertical drag. Among the three, the octocopter, with the largest surface area, consistently experiences the highest drag, while the quadcopter, being the most compact, experiences the least. This proportional trend remains consistent across all altitudes, indicating that for straightforward drone configurations, vertical drag can be reasonably estimated based on surface area alone. This also highlights that without complex aerodynamic structures, simpler drones maintain predictable aerodynamic behavior, making them more versatile and easier to optimize for missions that involve frequent altitude changes.

Finally, the graph once again demonstrates that vertical drag, being dependent on air density, decreases exponentially with increasing altitude, becoming effectively negligible around 50 km. Beyond this point, the aerodynamic inefficiencies of a drone's

design have little practical impact, as shown by the dramatic reduction in drag even for the typically inefficient VTOL design. However, it is important to emphasize that while drag becomes extremely small at such altitudes, it never truly reaches zero.

Overall, the data reveals clear differences in the performance of each drone design. To better illustrate these disparities, we can calculate the average values from each simulation, which will provide a representation of the overall performance in each category across various altitudes. These average values can then be presented in a table, allowing us to rank each design numerically for a more precise comparison. The table below shows these rankings.

	Avg horiz drag	Avg vert drag	Avg thrust	Mass	Avg thrust per kg
Quadcopter	8.164174768 N	19.19156579 N	40.51248515 N	5.7334 kg	7.06604737 N
Hexacopter	11.69910449 N	23.42516276 N	56.30801662N	7.3651 kg	7.645224031 N
Octocopter	10.52692989 N	27.14019104 N	59.89854567 N	9.0968 kg	6.584540674 N
VTOL	3.102676512 N	138.9794023 N	38.71901442 N	6.7739 kg	5.715875728 N

Table 5. Average performance of each drone

The table clearly demonstrates that no single drone design excels in all aspects, underscoring the importance of defining the intended purpose of the drone before selecting a specific model. For long-distance travel, the VTOL drone stands out as the superior choice due to its efficient horizontal motion. For tasks that require high vertical mobility and maneuverability, the quadcopter is ideal, offering reliability and simplicity. When maximum lifting power is crucial, particularly for carrying heavy payloads or performing demanding tasks, the octocopter is recommended. Lastly, for a balanced combination of power, weight, and efficiency, the hexacopter proves to be the best all-around option. Therefore, the optimal drone design depends on the specific requirements of the task at hand.

VTOL drones are ideally suited for long-distance travel within the same altitude layer, making them particularly effective for applications such as delivery or transportation. Their design, which prioritizes efficient horizontal motion, enables them to cover significant distances with minimal drag. This makes them an excellent choice for tasks that involve travelling over extended areas without the need for frequent altitude changes.

Quadcopters, on the other hand, are ideally suited for operations that require efficient vertical motion. With their ability to climb steadily to greater heights, they excel in applications that involve monitoring, surveillance, or measurements in elevated locations. Their relatively simple design, with four rotors providing balanced thrust, allows them to maneuver with precision in vertical flight, making them well-suited for

tasks such as environmental monitoring, infrastructure inspection, and aerial photography. The quadcopter's efficient lift capabilities make it particularly effective for scenarios where reaching specific altitudes is a priority.

Octocopters are especially useful in situations where maximum lift capacity is the primary concern, particularly at lower altitudes. With their eight rotors, octocopters can generate significantly more lift compared to drones with fewer motors, making them ideal for applications that require carrying heavy payloads. These include tasks such as cargo transport, aerial construction, and search-and-rescue operations, where the ability to lift and transport equipment or supplies is crucial. The additional rotors also provide increased stability, which is beneficial when operating in challenging conditions or carrying large loads.

Lastly, hexacopters are the most versatile and efficient drones overall. With the highest per-kilogram lift force among all drone types, they offer a balanced combination of power, stability, and efficiency. This makes them particularly well-suited for vertical transportation, such as in logistics and delivery services, where both payload capacity and energy efficiency are crucial. Additionally, their design allows for better performance at higher altitudes, making them ideal for applications in aerial surveying or environmental monitoring. The six rotors provide enhanced stability and redundancy, ensuring reliable flight even in challenging conditions. This versatility, combined with efficiency, positions hexacopters as a highly effective choice for a wide range of applications.

Effective range of thrusters:

This section will analyze the specific parameters and performance outputs of each thruster type—propeller-based, ion, and photon laser—across the different drone types. By evaluating how each propulsion system performs under various conditions, we will calculate the overall operational range of each drone. Through this comprehensive assessment, we aim to identify the best propulsion option for each altitude based on its intended use and performance characteristics.

Methods of assessment:

There are two primary methods for assessing the effective range of the thrusters. The first method, the safe range, involves determining the range based on the ability of the thrusters to overcome gravity and maintain stable flight. This is critical for understanding the altitude at which a drone can operate while still being able to counteract gravitational forces. The second method, the operational range, focuses on

utilizing orbital velocity to assess the drone's capability to reach and sustain higher altitudes, where it can maintain a stable orbit or perform long-duration missions. By evaluating both ranges, we can better understand the performance limitations and potential of each drone under different conditions.

The safe range refers to a zone where the thrusters of the drones are fully capable of overcoming the gravitational pull, allowing the drone to move freely and unhindered. In this range, the drone can achieve stable flight without being restricted by gravitational forces. This method of assessment is commonly employed by typical propeller-based drones, as their propulsion systems are designed to generate sufficient lift to counteract gravity and maintain controlled movement within this defined altitude zone.

Overcoming gravity is not the only way to maintain stable altitude in space. If an object reaches a high enough velocity, the gravitational force pulling it toward the planet can be counteracted by its speed, allowing the object to enter and remain in orbit rather than being pulled back down. This phenomenon is known as orbital velocity. The operational range refers to the point at which a drone can achieve and maintain sufficient thrust to reach and sustain orbital velocity, enabling it to remain at a fixed altitude. This method is commonly employed by satellites, which rely on achieving orbital velocity to maintain their position in space without the need for continuous thrust to counteract gravity.

Propeller-based thrusters:

The first type of thruster we will analyze is the propeller-based propulsion system, which is the most commonly used method in traditional drones. As previously discussed, this system generates thrust by creating pressure differences in the surrounding air, effectively pushing the drone forward or upward. In the earlier sections, we extensively examined the thrust characteristics and performance of propeller-driven drones across various conditions. Therefore, the data and findings from those discussions are directly applicable to this section, providing a foundation for evaluating the propeller system’s operational capabilities.

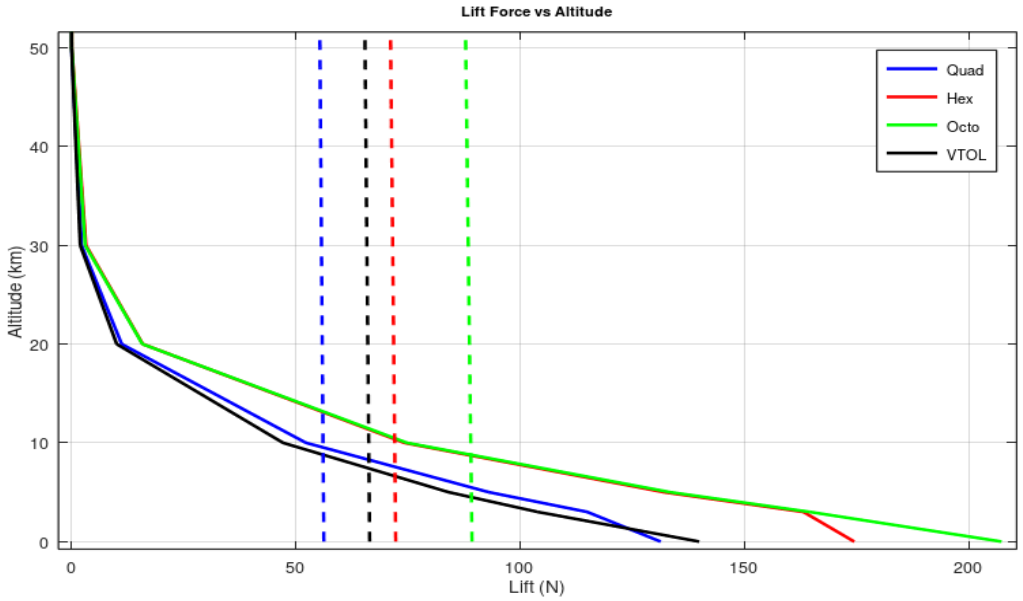

Figure 26. Lift and gravitational force vs altitude

The graph above illustrates the lift generated by each drone, represented by solid lines, and the corresponding gravitational force, represented by dashed lines, as a function of altitude. We observe that for each drone, there is a specific altitude at which these two forces intersect, meaning the lift produced becomes equal to the gravitational pull. This intersection point varies depending on the drone type. For example, the VTOL drone reaches this limit at approximately 7.4 km, while the hexacopter achieves the highest safe range at around 10.3 km. These points define the maximum altitude, or safe range, for each propeller-based drone. Beyond this altitude, the thrust produced by the propellers is no longer sufficient to overcome gravity, making sustained flight impossible.

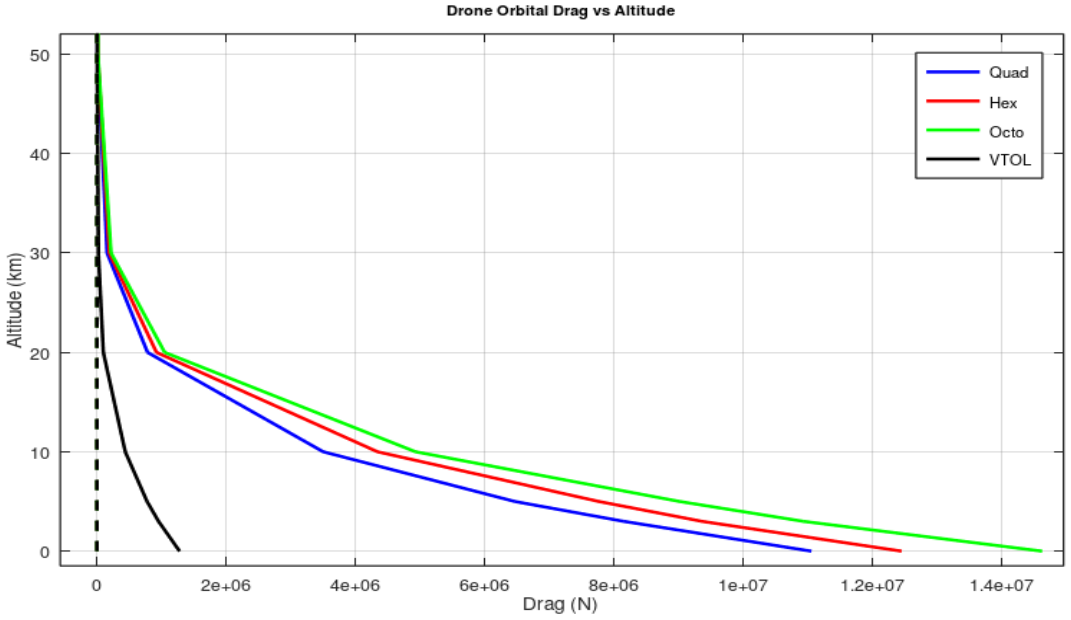

Figure 27. Lift and orbital drag vs altitude

The graph above depicts the air resistance encountered when moving at orbital velocity at various altitudes, represented by solid lines, and the thrust produced by each drone, represented by dashed lines. At lower altitudes, where air density is highest, travelling at orbital velocity generates extreme levels of drag, reaching into the multi-meganewton range. This immense force is not only far beyond what the drones' thrusters can produce, but it would also immediately destroy the drone, making orbital flight at these altitudes completely unfeasible. Although the drag decreases dramatically with increasing altitude, the thrust generated by the propellers also diminishes. As a result, propeller-based drones are never able to produce enough force to maintain orbital velocity at any altitude, firmly limiting their application to low-altitude operations.

Propeller	Mass (kg)	Force (N)	Safe range (km)	Operational range (km)
Quadcopter	5.733401296	56.098	0 - 9.5297	unfeasible
Hexacopter	7.365123166	72.044	0 - 7.4055	unfeasible
Octocopter	9.096844964	89.028	0 - 10.368	unfeasible
VTOL	6.773942658	66.323	0 - 8.7856	unfeasible

Table 6. Effective range of propellers

Overall, we observe that propeller-based thrusters are the most reliable form of propulsion for lower altitudes, maintaining effective operation up to approximately 10 kilometers depending on the drone model. However, they have no capability to achieve or sustain orbital velocities, meaning they are unsuitable for continuous use in space or at very high altitudes. As a result, propeller-based systems are best utilized for short, controlled bursts of motion within the atmosphere, where their thrust can be fully effective.

Simulation limitations:

As we move on to analyze the next two propulsion methods, it becomes critically important for the results to be extremely precise due to the relatively low forces produced by these thrusters. However, it is important to note that both the environmental simulation provided by JB2008 and the CFD simulation conducted using Ansys Fluent become increasingly unreliable at extremely low air densities, particularly beyond altitudes of 1000 km. This introduces a limitation in the accuracy of the analysis at very high altitudes and should be taken into consideration when interpreting the results.

Fortunately, since we have gathered ample data from our previous simulations, we can estimate the required values by extrapolating from known data points. For instance, by using the known air density value at 1000 km, we can reasonably project the air density at higher altitudes, such as 1500 km. While this method introduces a degree of approximation, it allows us to extend our analysis beyond the limitations of the simulation tools and continue evaluating the performance of the propulsion methods across greater altitudes. We can extrapolate air densities using the barometric formula:

$$\rho_{(h)} = \rho_0 e^{\frac{-gM(h-h_0)}{RT}} \quad (6)$$

$\rho_{(h)}$ = density at altitude h (in kg/m³)

ρ_0 = known density at reference altitude h_0 (kg/m³)

h = altitude where you want to estimate the density (km)

h_0 = reference altitude (km)

M = molar mass of air (kg/mol)

g = gravitational acceleration (m/s²)

R = universal gas constant (J/mol·K)

T = absolute temperature (K)

Estimating the resultant drag force without the aid of simulation is significantly more challenging, as it involves many variables that are difficult to determine precisely, such as the exact area of contact and drag constant. Drag force is calculated using the following formula:

$$F_D = \frac{1}{2}\rho v^2 C_D A \quad (7)$$

F_D = Drag force (N)

ρ = Fluid density (kg/m³)

v = Relative velocity (m/s)

C_D = Drag coefficient

A = Reference area (m²)

While we can determine the air density using the barometric formula and calculate the relative velocity through orbital velocity, the exact contact area and drag coefficient remain unknown. Fortunately, since these unknowns behave as constants for each drone, we can estimate their combined effect by deriving a single multiplicative

constant based on the simulation results. Using the available data, the approximate values for each drone are as follows:

	Density (kg/m³)	Orbital velocity (m/s)	Drag (N)	1/2*A*C(D)
Quadcopter	1.225	7909.6808	11048900	0.144166727
Hexacopter	1.225	7909.6808	12445000	0.1623831257
Octocopter	1.225	7909.6808	14619100	0.1907509163
VTOL	1.225	7909.6808	1277090	0.0166635489

Table 7. Drag coefficient of each drone

To verify the accuracy of these values, the same calculation method was applied across all simulation results. A detailed table containing the full calculations can be found in the appendix. This approach not only helps validate our estimates but also highlights the exact limitations of the simulation, indicating where errors begin to accumulate. Based on the results, it was observed that beyond approximately 80 km in altitude, the air density becomes too low for the simulations to remain reliably accurate.

Finally, by applying these methods, we are able to reliably estimate even the smallest forces with a high degree of accuracy. This approach enables us to accurately determine the operational ranges of the remaining two thruster types, despite the strict limitations and decreasing reliability of our simulation at higher altitudes.

Ion thrusters:

The next type of thruster we will analyze is the ion-based propulsion system, which presents intriguing possibilities for drone and high-altitude applications. As previously discussed, ion thrusters generate thrust by electrically accelerating charged particles (ions) through an electric field, producing a high-velocity ion beam that propels the vehicle forward. In the earlier sections, we explored the design, working principles, and thrust characteristics of ion propulsion systems, where we calculated that each thruster would produce approximately $T_i = 0.0264N$. In this section, we will evaluate the operational capabilities of ion thrusters in near-space or vacuum conditions using the method previously discussed.

Determining the safe range for drones equipped with ion thrusters is relatively straightforward. Since these thrusters produce a constant force that is independent of external factors like altitude or air density, we can directly calculate the altitude at which the gravitational pull equals the thrust generated by each drone. Using Newton's law of universal gravitation $F = \frac{GMm}{(R+h)^2}$, we can find the precise point where these forces balance. Based on these calculations, the safe range for the drones is found to be

approximately 200,000 kilometers. This altitude lies well within the region known as high Earth orbit, far beyond the typical operational range of most satellites.

To determine the operational range of ion thrusters, we need to apply the extrapolation method discussed earlier. Since the thrust produced by the ion thrusters is known and constant, we can rearrange the drag force equation to solve for the required air density at which the generated thrust would balance the drag force experienced at orbital velocity. Once the corresponding air density is found, we can then use the inverse of the barometric formula to calculate the corresponding altitude. The calculation process looks like this:

$$\rho = \frac{2F_D}{v^2 C_D A} \rightarrow h = h_0 - \frac{RT}{gM} ln(\frac{\rho}{\rho_0}) \quad (8)$$

This two-step process, first finding the critical air density and then determining the corresponding altitude, allows us to accurately estimate the operational range of ion thrusters, even beyond the reliable limits of direct simulation. Using this method, we find that the operational range of ion thrusters is significantly lower compared to their safe range, with effective operation extending only up to around 550 kilometers. This places ion thrusters firmly within low Earth orbit, making them suitable for applications that require sustained operation in these lower orbital regions.

Ion	Mass (kg)	Force (N)	Safe range (km)	Operational range (km)
Quadcopter	10.3905441	0.1056	198040+	536.9865+
Hexacopter	14.35083737	0.1584	190030+	530.1+
Octocopter	18.41113056	0.2112	186400+	526+
VTOL	12.59537116	0.1056	218040+	540.5+

Table 8. Effective range of ion thrusters

Ion thrusters are highly versatile, capable of operating effectively in LEO (low Earth orbit) and beyond. Their ability to function in these environments, combined with their exceptionally high efficiency, makes them one of the most effective forms of propulsion discussed in this study. Although their thrust is relatively low compared to traditional propeller-based systems, their continuous and efficient operation over long periods allows for sustained maneuvering and positioning, making them ideal for long-duration space missions and satellite propulsion.

Photon laser thrusters:

Finally, the last type of thruster we will analyze is PLT, which offers exciting prospects for high-altitude and space-based applications. Photon laser thrusters operate by using high-powered laser beams to propel a vehicle forward. The laser energy is absorbed by the vehicle's reflective surface, generating a reactive force in the opposite direction according to Newton's Third Law of Motion. This type of propulsion system is extremely efficient, as it doesn't require traditional fuel and can potentially operate for extended periods. In earlier sections, we discussed the principles behind photon laser propulsion and the energy requirements and calculated the thrust to be $T_i = 3.3333\mu N$. In this section, we will once again evaluate the operational capabilities of photon laser thrusters in near-space or vacuum conditions. The calculation method and approach used for photon laser thrusters are identical to those for ion thrusters, so we will not repeat the process here.

The safe range of PLTs begins extremely far, at 16,589,000 km, which is almost 50 times the distance from Earth to the moon. This range places the PLTs well beyond high Earth orbit, far outside the operational range of any existing devices. Fortunately, since PLTs operate entirely using internal electrical power, which can be continuously supplied by solar energy, they do not require refuelling. This makes them perfectly operational at such high altitudes.

The operational range of PLTs suggests that they are capable of reaching altitudes as low as 800 kilometers, which would place them within LEO. However, it is important to note that due to their relatively low thrust capabilities and extended recharge times, utilizing PLTs at such low altitudes could be risky. These factors make it challenging to maintain efficient and safe operations in LEO. As a result, PLTs are better suited for missions in medium Earth orbit (MEO) or high Earth orbit (HEO), where the advantages of their high efficiency and long-duration propulsion systems can be fully realized without the limitations posed by lower altitudes

PLT	Mass (kg)	Force (N)	Safe range (km)	Operational range (km)
Quadcopter	10.3905441	0.000013333332	17,624,000+	799.7+
Hexacopter	14.35083737	0.000019999998	16,912,000+	792.8+
Octocopter	18.41113056	0.000026666664	16,589,000+	788.7+
VTOL	12.59537116	0.000013333332	19,404,000+	803.2+

Table 9. Effective range of PLT

Finally, PLTs present a unique case in propulsion technology. Their mode of operation eliminates the need for resupply, granting them the potential for extremely

long-range missions, far surpassing the reach of other thrusters discussed in this study. However, their very low thrust forces significantly limit their practical applications, restricting their use primarily to HEO. As technology continues to advance, the greatest advantage of PLTs lies in their ability to operate indefinitely in deep space regions without the need for refueling, making them a promising option for long-duration space missions.

Chapter 5: Conclusion

Over the course of the study, we have discussed 4 distinct types of drones: quadcopter, hexacopter, octocopter, and VTOL. We found, through extensive research, that when performing in high altitude conditions, each design excelled in different factors: quadcopters being most efficient at vertical flight, VTOLs most efficient at horizontal flight, and octocopters having the highest overall carrying capacity. However, the hexacopter, performing effectively in all parameters and having the highest lift force per kg, emerged as the best design for general purposes.

Through our assessment of the 3 thruster types, we found the limitations and operational range of each and their ideal usages. Traditional propeller-based thrusters provide the highest thrust; however, due to their dependency on air density, they cannot be deployed in orbital operations, instead being limited to on-demand missions in low altitude. Ion thrusters provide the most promising result, being able to operate well within LEO and beyond; they would be the primary candidate for orbital drones. Despite being in very early experimental phases, the study proves that PLTs can be operational in MEO to HEO ranges; however, their most exciting potential is in deep-space, off-world applications.

The main focus of this thesis has been building a reliable simulation model to assess and calculate the aerodynamic efficiency, thrust output, and overall performance of the drones. Since the research was based mostly on relative research by comparing different drone and thruster types, exact parametric values weren't as important. However, if the model is to be used to construct physical drones, each and every parameter discussed in this paper needs to be finely tuned and calibrated. Therefore, future research regarding this topic should focus more on the physical implementation of these concepts by testing for a specific case to fine-tune and apply the simulation to real-world scenarios.

References:

(1) Piesing M. The Secret History of Drones [Internet]. Si.edu. 2024. Available from: https://airandspace.si.edu/air-and-space-quarterly/issue-12/secret-history-of-drones

(2) Skobelev S, Skobelev S. Approach to Evaluation of the Application and Efficiency of Stratosphere UAV. ResearchGate [Internet]. 2021 Oct [cited 2025 Apr 29]. Available from: https://www.researchgate.net/publication/355690823_APPROACH_TO_EVALUATION_OF_THE_APPLICATION_AND_EFFICIENCY_OF_STRATOSPHERE_UAV

(3) You K, Zhao X, Zhao S-Z, Faisal M. Design and Optimization of a High-Altitude Long Endurance UAV Propeller. IOP Conference Series: Materials Science and Engineering. 2020 Sep 25;926:012018.

(4) Reid WA, Albayati IM. Design of an unmanned aircraft system for high-altitude 1 kW fuel cell power system. Aerospace Systems. 2021 Oct 22;4(4):353–63.

(5) Kirsch B, Olivier Montagnier. Towards the Advent of High-Altitude Pseudo-Satellites (HAPS). HAL (Le Centre pour la Communication Scientifique Directe) [Internet]. 2019 Jul 8 [cited 2025 Apr 29];181–201. Available from: https://www.researchgate.net/publication/335604911_Towards_the_Advent_of_High-Altitude_Pseudo-Satellites_HAPS

(6) FAA. Forces Acting on the Aircraft Aerodynamics of Flight [Internet]. 2023 Jul. Available from: https://www.faa.gov/sites/faa.gov/files/07_phak_ch5_0.pdf

(7) Reid J. Drone flight -what does basic physics say? [Internet]. 2018. Available from: https://homepages.abdn.ac.uk/nph120/meteo/DroneFlight.pdf

(8) STUDY OF PROPELLER DESIGN PARAMETERS | International Journal of Innovations in Engineering Research and Technology [Internet]. Ijiert.org. 2015. Available from: https://repo.ijiert.org/index.php/ijiert/article/view/740?utm

(9) Scholze F, F. Pietag, Adirim H, Kreil M, Kron M, Woyciechowski R, et al. Development and test of a cost-efficient gridded ion thruster propulsion system for small satellites – IonJet. Journal of Electric Propulsion. 2022 Dec 1;1(1).

(10) Huang Q, Jin X, Ye J. The theory modeling analysis of photonic laser propulsion based on oscillation in external cavity. Jin W, Li Y, editors. Fourth Seminar on Novel Optoelectronic Detection Technology and Application. 2018 Feb 20;48.

(11) U.S. Standard Atmosphere, 1976. Washington (DC): U.S. Government Printing Office; 1976. NOAA, NASA, USAF.

(12) Bowman BR, Tobiska WK, Marcos FA, Huang CY, Lin CH, Burke WJ. A new empirical thermospheric density model JB2008 using new solar and geomagnetic indices. AIAA/AAS Astrodynamics Specialist Conference and Exhibit; 2008 Aug 18–21; Honolulu, Hawaii. Reston (VA): AIAA; 2008. Report No.: AIAA 2008-6438.

(13) ANSYS®, Inc. ANSYS Fluent Academic Research, Release 2024 R2. Computational Fluid Dynamics Software. Canonsburg (PA): ANSYS, Inc.; 2024.

(14) GRC - NSTAR [Internet]. web.archive.org. 2003. Available from: https://web.archive.org/web/20030111164356/http://www.grc.nasa.gov/WWW/ion/past/90s/nstar.htm

APPENDIX A: List of Figures, Tables and Formulas

List of figures:

List of tables:

List of formulas:

Quadcopter engineering drawing

APPENDIX B: Engineering Drawings

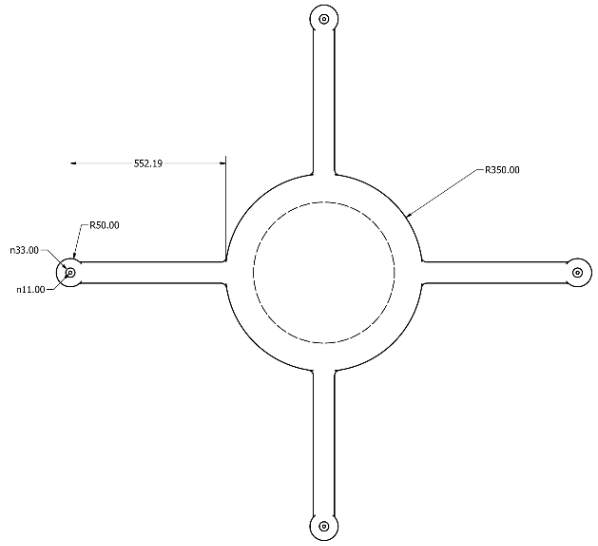

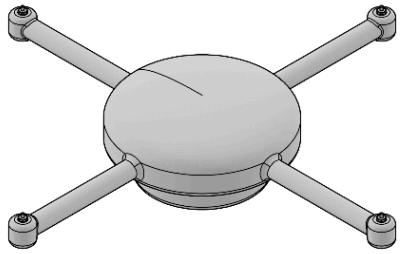

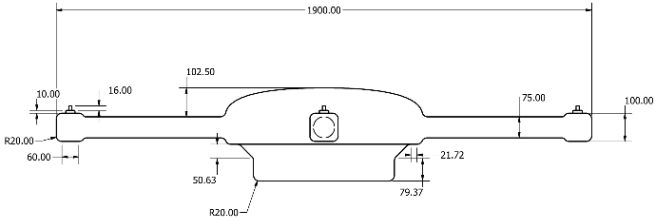

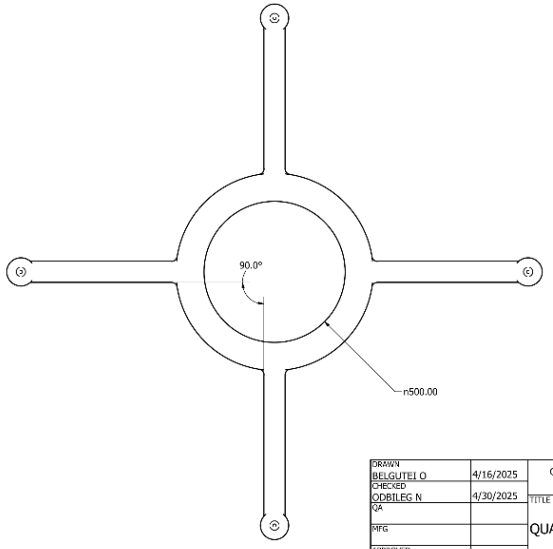

DRAWN BELGUTEI O	4/16/2025	GERMAN MONGOLIAN INSTITUTE OF RESOURCES AND TECHNOLOGY	
CHECKED ODBILEG N	4/30/2025	TITLE	
QA		QUADCOPTER DESIGN	
MFG			
APPROVED ODBILEG N	4/30/2025	SIZE D / DWG NO QUADCOPTER / REV 1	
		SCALE 1 / 8	SHEET 1 OF 1

Hexacopter engineering drawing

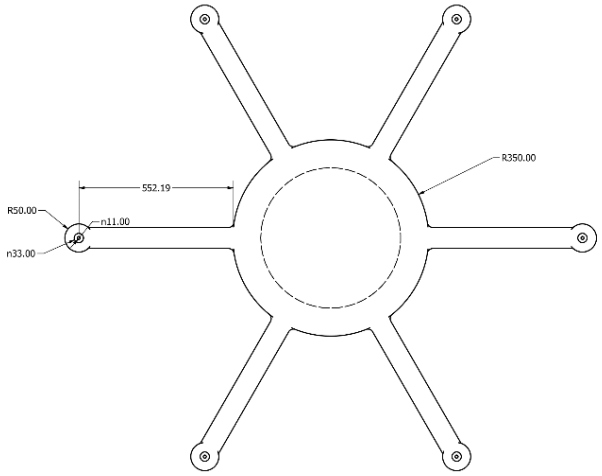

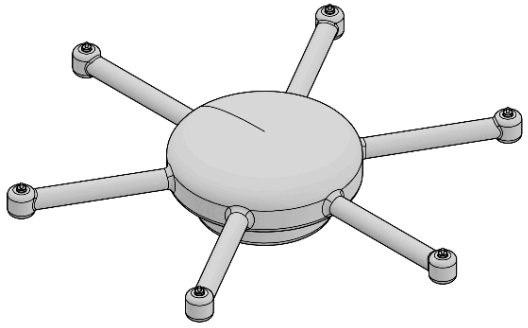

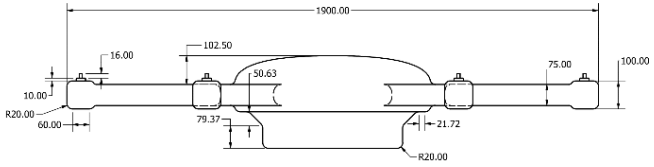

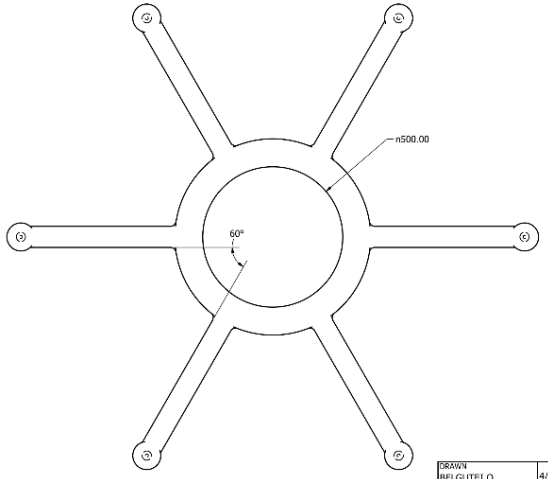

DRAWN BELGUTEI O	4/16/2025	GERMAN MONGOLIAN INSTITUTE OF RESOURCES AND TECHNOLOGY	
CHECKED ODBILEG N	4/30/2025	TITLE	
QA			
MFG		HEXCOPTER DESIGN	
APPROVED ODBILEG N	4/30/2025	SIZE D	DWG NO HEXCOPTER
		SCALE 1 / 8	REV 1
			SHEET 1 OF 1

Octocopter engineering drawing

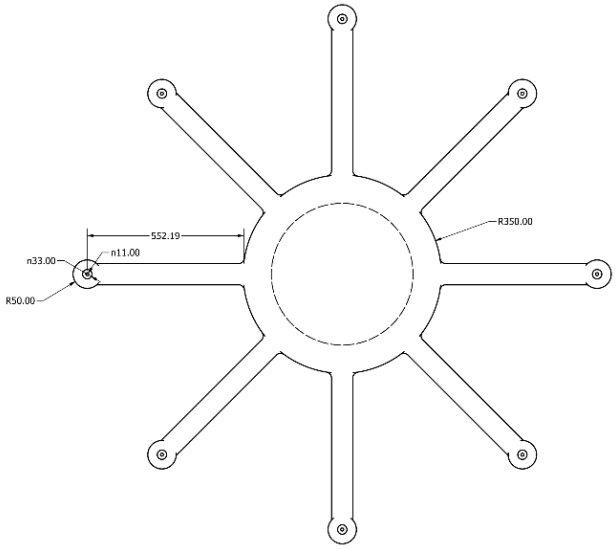

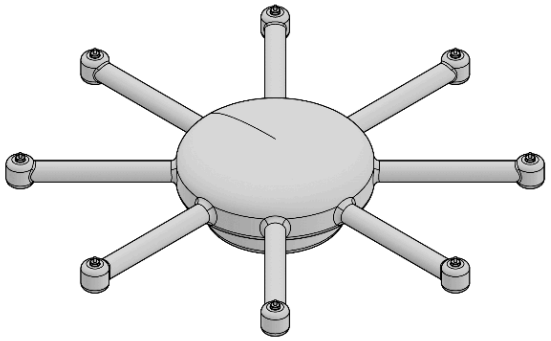

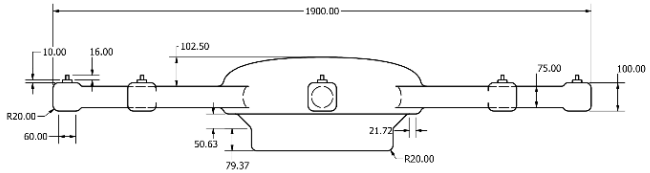

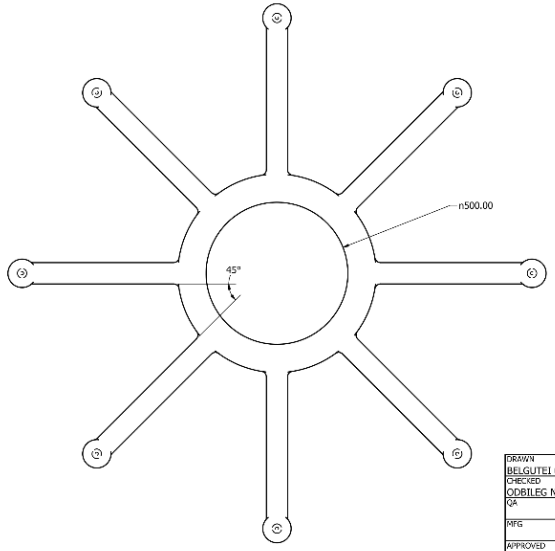

DRAWN BELGUTEI O	4/16/2025	GERMAN MONGOLIAN INSTITUTE OF RECOURSES AND TECHNOLOGY	
CHECKED ODBILEG N	4/30/2025	TITLE	
QA		OCTOCOPTER DESIGN	
MFG			
APPROVED ODBILEG N	4/30/2025	SIZE D	DWG NO OCTOCOPTER
		SCALE 1 / 8	REV 1
		SHEET 1 OF 1	

VTOL engineering drawing

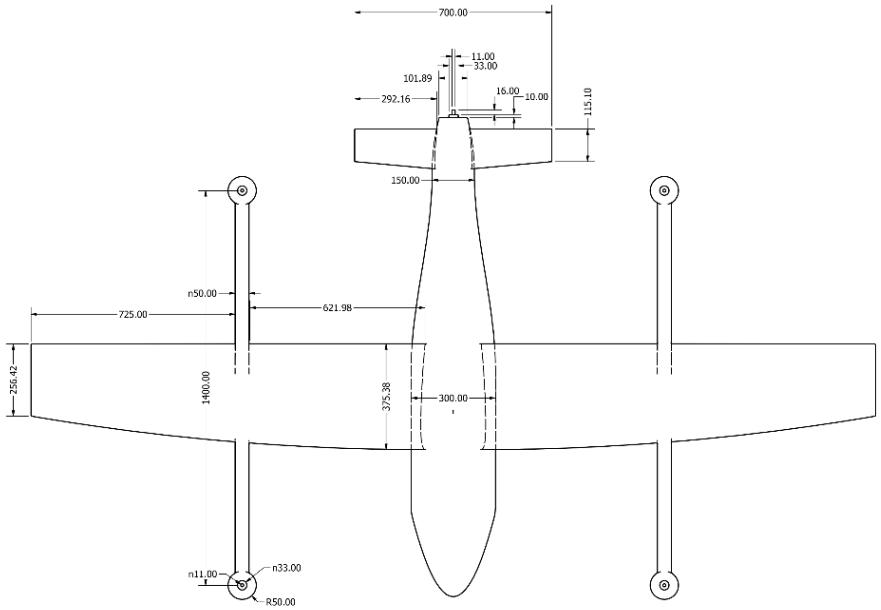

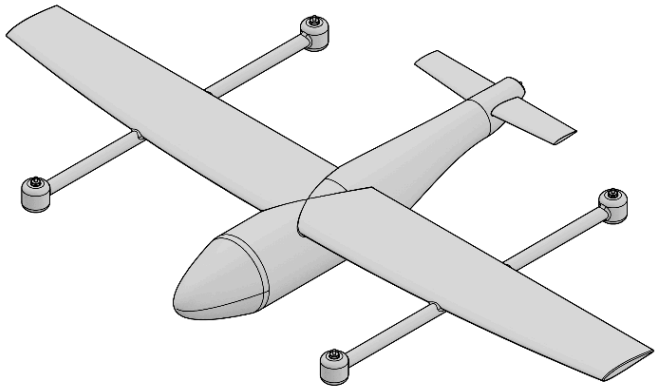

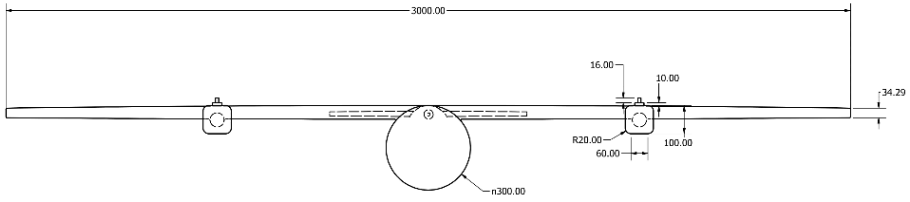

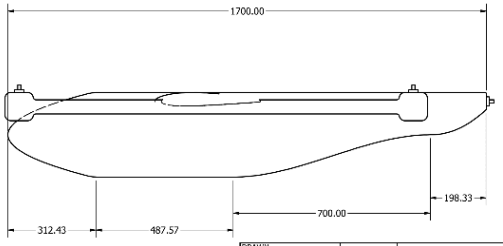

DRAWN BELGUTEI O	4/16/2025	GERMAN MONGOLIAN INSTITUTE OF RESOURCES AND TECHNOLOGY	
CHECKED ODBILEG N	4/30/2025	TITLE	
QA		VTOL DRONE DESIGN	
MFG			
APPROVED ODBILEG N	4/30/2025	SIZE D / DWG NO VTOL DRONE / REV 1	
		SCALE 1/8	SHEET 1 OF 1

Propeller engineering drawing

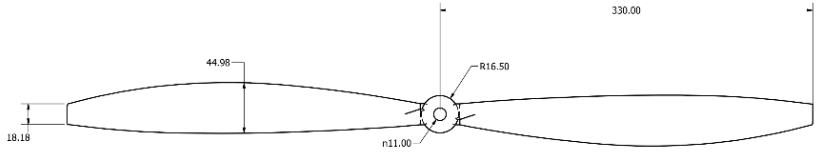

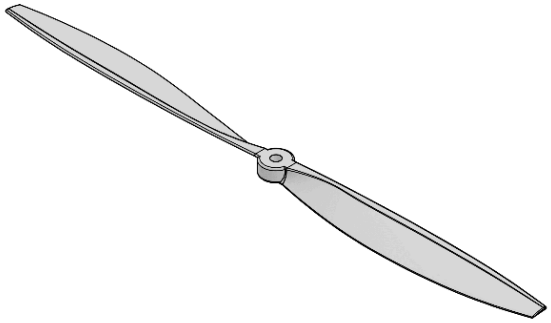

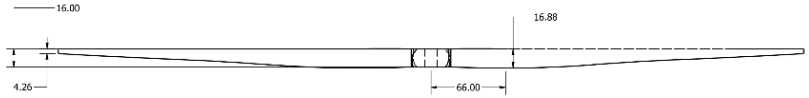

DRAWN BELGUTEI O	4/16/2025	GERMAN MONGOLIAN INSTITUTE OF RESOURCES AND TECHNOLOGY	
CHECKED ODBILEG N	4/30/2025	TITLE	
QA		PROPELLER DESIGN	
MFG			
APPROVED ODBILEG N	4/30/2025	SIZE D / DWG NO PROPELLER / REV 1	
		SCALE 1 / 2	SHEET 1 OF 1

APPENDIX C: Tables

VTOL simulation data

Altitude (km)	Density (kg/m3)	Viscosity (Pa*s)	Horizontal Drag (N)	Vertical Drag (N)	Body Drag (N)	Thruster1 (N)	Thruster2 (N)	Thruster3 (N)	Thruster4 (N)	Lift (N)
0	1.225	0.000017894	-10.7187	-500.141	-15.2892	36.5108	39.943	39.1416	39.5464	139.8526
3	0.90917	0.000016938	-8.14571	-371.798	-11.317	27.1662	29.6385	29.0737	29.3514	103.9128
5	0.73634	0.000016283	-6.70626	-301.49	-9.1693	21.9184	24.0366	23.5255	23.7649	84.0761
10	0.41349	0.000014577	-3.94963	-170.004	-5.20401	12.3282	13.4805	13.2329	13.3401	47.17769
20	0.08891	0.000014215	-1.04533	-37.3958	-1.11662	2.65492	2.88612	2.82452	2.86272	10.11166
30	0.01841	0.000014752	-0.336298	-8.19243	-0.241503	0.532687	0.569751	0.560318	0.570198	1.991451
50	0.0010268	0.000017036	-0.0831568	-0.638647	-0.0200955	0.0208586	0.0220955	0.0210029	0.0224016	0.0662631
80	0.000018456	0.000013208	-0.0143981	-0.0412662	0.000202034	0.0000726547	-0.0000487624	-0.0000208213	-0.00000972085	0.00019538415
100	0.00000068458	0.000013046	9.80E-05	-0.0253136	0.000438203	0.000102	-0.0000212928	0.0000202163	0.0000303811	0.0005695076
200	0.00000000025408	0.000037743	-0.0273802	-0.0675666	-0.0000353147	0.000053784	0.000288521	0.000259353	0.000248822	0.0008151653

Quadcopter simulation data

Altitude (km)	Density (kg/m3)	Viscosity (Pa*s)	Horizontal Drag (N)	Vertical Drag (N)	Body Drag (N)	Thruster1 (N)	Thruster2 (N)	Thruster3 (N)	Thruster4 (N)	Lift (N)
0	1.225	0.000017894	-28.6775	-68.2863	-6.2971	34.555	34.7809	33.262	34.9729	131.2737
3	0.90917	0.000016938	-21.5892	-50.9056	-4.73024	32.0786	31.9852	33.3141	22.298	114.94566
5	0.73634	0.000016283	-17.7716	-41.5129	-3.88663	25.9803	25.8958	26.9643	18.0774	93.03117
10	0.41349	0.000014577	-10.3192	-23.9256	-2.16338	14.5719	14.5424	15.1601	10.1611	52.27212
20	0.08891	0.000014215	-2.5498	-5.58971	-0.443866	3.12653	3.11454	3.25517	2.17626	11.228634
30	0.01841	0.000014752	-0.621193	-1.43659	-0.0771163	0.634094	0.628838	0.658729	0.438318	2.2828627
50	0.0010268	0.000017036	-0.079572	-0.193427	-0.00138205	0.0247187	0.0217734	0.0246652	0.0129171	0.08269235
80	0.000018456	0.000013208	-0.00910493	-0.0192093	-0.00136664	0.00055674	0.000820271	0.000440832	0.000566786	0.001017989
100	0.00000068458	0.000013046	-0.00686765	-0.0130672	0.0021873	0.00036394	0.000376705	0.00021033	0.00101731	0.004155585
200	0.000000000254	0.000037743	-0.0177101	-0.0332544	-0.0024147	0.00110428	0.00160203	0.000914891	0.00163233	0.002838831

Octocopter simulation data

Altitude (km)	Density (kg/m3)	Viscosity (Pa*s)	Horizontal Drag (N)	Vertical Drag (N)	Body Drag (N)	Thruster1 (N)	Thruster2 (N)	Thruster3 (N)	Thruster4 (N)	Thruster5 (N)	Thruster6 (N)	Thruster7 (N)	Thruster8 (N)	Lift (N)
0	1.225	0.000017894	-37.2945	-96.5876	-19.6621	28.9553	25.3843	29.1082	29.0322	28.5979	27.0628	29.7817	28.9496	207.2099
3	0.90917	0.000016938	-27.923	-72.1773	-14.676	25.2144	13.9334	26.1674	22.4083	25.4245	15.6196	26.2915	24.1521	164.5352
5	0.73634	0.000016283	-22.7775	-58.669	-11.779	20.4225	11.292	21.2251	18.1913	20.585	12.6285	21.2667	19.5738	133.4059
10	0.41349	0.000014577	-13.0305	-33.6516	-6.69855	11.4359	6.39784	11.9066	10.2288	11.5356	7.0679	11.9477	10.9696	74.79139
20	0.08891	0.000014215	-3.23112	-7.92452	-1.43226	2.41426	1.31535	2.55	2.18868	2.43981	1.48008	2.55761	2.33291	15.84644
30	0.01841	0.000014752	-0.858105	-2.03914	-0.270523	0.474133	0.235307	0.513541	0.440108	0.465829	0.266314	0.506281	0.465912	3.096902
50	0.0010268	0.000017036	-0.1117	-0.265163	-0.0245212	0.0192143	0.00387828	0.0166593	0.0167322	0.0192381	0.00403531	0.018979	0.0175933	0.09180859
80	0.000018456	0.000013208	-0.0118521	-0.026345	-0.00140302	-0.0000108082	0.00133413	0.001072	-0.00115032	0.000115473	0.00150809	0.000249887	-0.0000160196	0.0016994122
100	0.00000068458	0.000013046	-0.00855919	-0.0172819	0.000619563	-0.0000901061	0.00210771	0.00752055	-0.00533839	-0.0001038	0.00119986	0.000240166	0.0000611123	0.0062166652
200	0.00000000025408	0.000037743	-0.0224626	-0.0439605	unstable	unstable	unstable	unstable	unstable	unstable	unstable	unstable	unstable	0

Hexacopter simulation data

Altitude (km)	Density (kg/m3)	Viscosity (Pa*s)	Horizontal Drag (N)	Vertical Drag (N)	Body Drag (N)	Thruster1 (N)	Thruster2 (N)	Thruster3 (N)	Thruster4 (N)	Thruster5 (N)	Thruster6 (N)	Lift (N)
0	1.225	0.000017894	-41.9907	-83.4435	-7.92191	29.0772	31.4402	28.1088	31.0522	31.6843	30.9717	174.41249
3	0.90917	0.000016938	-31.1783	-62.1808	-5.82897	21.8898	31.3354	21.4547	31.4178	32.0653	30.7978	163.13183
5	0.73634	0.000016283	-25.2721	-50.6609	-4.81392	17.8021	25.3101	17.3844	25.4362	25.9594	24.9488	132.02708
10	0.41349	0.000014577	-14.3499	-29.1034	-2.68347	9.99192	14.2365	9.75394	14.2838	14.5546	14.0488	74.18609
20	0.08891	0.000014215	-3.27439	-6.83282	-0.568445	2.1216	3.05402	2.09762	3.06466	3.12517	3.02242	15.917045
30	0.01841	0.000014752	-0.78902	-1.73175	-0.115227	0.446442	0.622734	0.437959	0.625841	0.639167	0.620005	3.276921
50	0.0010268	0.000017036	-0.0982462	-0.224847	-0.00370939	0.0094037	0.0252197	0.00947436	0.0263024	0.0249877	0.0256442	0.11732267
80	0.000018456	0.000013208	-0.0105829	-0.0219767	-0.00167795	0.0016829	0.000221231	0.00175806	-0.000079977	-0.000117463	0.000113279	0.00190008
100	0.00000068458	0.000013046	-0.00771394	-0.0145599	0.0012138	0.00119827	0.000198071	0.00128634	0.0000515783	0.0000979106	0.000104723	0.0041506929
200	0.00000000025408	0.000037743	-0.0200919	-0.037074	-0.00383325	0.0042647	0.000411051	0.00432134	-0.0000116551	-0.000083237	0.000267776	0.0053367249

Orbital drag simulation data

Altitude (km)	Density (kg/m3)	Viscosity (Pa*s)	Orbital velocity (m/s)	Quadcopter drag (N)	Hexcopter drag (N)	Octocopter drag (N)	VTOL drag (N)
0	1.225	0.000017894	7909.6808	-11048900	-12445000	-14619100	-1277090
3	0.90917	0.000016938	7907.8192	-8147570	-9357850	-10926400	-951797
5	0.73634	0.000016283	7906.5789	-6462360	-7761840	-9011560	-774287
10	0.41349	0.000014577	7903.4806	-3499690	-4339770	-4927280	-436875
20	0.08891	0.000014215	7897.2948	-782112	-920218	-1046760	-97937.8
30	0.01841	0.000014752	7891.1236	-156553	-190696	-217659	-21456.2
50	0.0010268	0.000017036	7878.8245	-9255.81	-11129.7	-13081.2	-1553.01
80	0.000018456	0.000013208	7860.4831	-280.879	-334.434	-394.157	-81.1088
100	0.00000068458	0.000013046	7848.3265	-26.9809	-31.2581	-37.0012	-13.7819
200	0.00000000025408	0.000037743	7788.3781	-14.6174	-16.2666	-19.3031	-12.0816
400	0.0000000000028041	0.000041416	7672.4904	-14.6997	-16.3344	-19.339	-12.2339
700	0.000000000000030732	0.000041519	7507.9668	-10.6497	-12.0764	-14.2325	-7.84873
1000	0.0000000000000036115	0.000041520	7353.5924	-7.4566	-8.6757	-10.2501	-4.35079

Drag coefficient calculation

	Density (kg/m3)	Orbital velocity (m/s)	Drag (N)	1/2*A*C(D)		Density (kg/m3)	Orbital velocity (m/s)	Drag (N)	1/2*A*C(D)
Quadcoper	1.225	7909.6808	-11048900	-0.144166727	Octocopter	1.225	7909.6808	-14619100	-0.1907509163
	0.90917	7907.8192	-8147570	-0.143307705		0.90917	7907.8192	-10926400	-0.1921845787
	0.73634	7906.5789	-6462360	-0.1403897938		0.73634	7906.5789	-9011560	-0.1957692005
	0.41349	7903.4806	-3499690	-0.1354964081		0.41349	7903.4806	-4927280	-0.1907679656
	0.08891	7897.2948	-782112	-0.1410462807		0.08891	7897.2948	-1046760	-0.1887729696
	0.01841	7891.1236	-156553	-0.1365620143		0.01841	7891.1236	-217659	-0.189865103
	0.0010268	7878.8245	-9255.81	-0.1452130735		0.0010268	7878.8245	-13081.2	-0.2052290677
	0.000018456	7860.4831	-280.879	-0.2463106624		0.000018456	7860.4831	-394.157	-0.3456473134
	0.00000068458	7848.3265	-26.9809	-0.6398498926		0.00000068458	7848.3265	-37.0012	-0.8774805083
	0.00000000025408	7788.3781	-14.6174	-948.4306859		0.00000000025408	7788.3781	-19.3031	-1252.456139
	0.0000000000028041	7672.4904	-14.6997	-89051.71069		0.0000000000028041	7672.4904	-19.339	-117156.883
	0.000000000000030732	7507.9668	-10.6497	-6147547.066		0.000000000000030732	7507.9668	-14.2325	-8215720.97
	0.0000000000000036115	7353.5924	-7.4566	-38181599.66		0.0000000000000036115	7353.5924	-10.2501	-52485746.14
Hexacopter	1.225	7909.6808	-12445000	-0.1623831257	VTOL	1.225	7909.6808	-1277090	-0.0166635489
	0.90917	7907.8192	-9357850	-0.1645953342		0.90917	7907.8192	-951797	-0.01674116868
	0.73634	7906.5789	-7761840	-0.168619996		0.73634	7906.5789	-774287	-0.01682078874
	0.41349	7903.4806	-4339770	-0.1680215239		0.41349	7903.4806	-436875	-0.01691435335
	0.08891	7897.2948	-920218	-0.1659523526		0.08891	7897.2948	-97937.8	-0.01766212823
	0.01841	7891.1236	-190696	-0.1663451348		0.01841	7891.1236	-21456.2	-0.01871635735
	0.0010268	7878.8245	-11129.7	-0.1746122645		0.0010268	7878.8245	-1553.01	-0.0243649508
	0.000018456	7860.4831	-334.434	-0.2932745419		0.000018456	7860.4831	-81.1088	-0.07112657854
	0.00000068458	7848.3265	-31.2581	-0.7412833496		0.00000068458	7848.3265	-13.7819	-0.3268366598
	0.00000000025408	7788.3781	-16.2666	-1055.436849		0.00000000025408	7788.3781	-12.0816	-783.8986533
	0.0000000000028041	7672.4904	-16.3344	-98954.82649		0.0000000000028041	7672.4904	-12.2339	-74113.7386
	0.000000000000030732	7507.9668	-12.0764	-6971110.678		0.000000000000030732	7507.9668	-7.84873	-4530685.098
	0.0000000000000036115	7353.5924	-8.6757	-44424014.18		0.0000000000000036115	7353.5924	-4.35079	-22278266.5

Mass distribution table

Propeller	Volume (mm^3)	Frame mass (kg)	Propulsion (kg)	Electrical pack (kg)	Total (kg)
Quadcoper	106004337.7	2.333401296	1.2	2.2	5.733401296
Hexacopter	111988344.6	2.465123166	1.8	3.1	7.365123166
Octocopter	117972348.3	2.596844964	2.4	4.1	9.096844964
VTOL	116931917	2.573942658	1.5	2.7	6.773942658

Ion	Volume (mm^3)	Frame mass (kg)	Propulsion (kg)	Electrical pack (kg)	Total (kg)
Quadcoper	106004337.7	2.333401296	5.8571428	2.2	10.3905441
Hexacopter	111988344.6	2.465123166	8.7857142	3.1	14.35083737
Octocopter	117972348.3	2.596844964	11.7142856	4.1	18.41113056
VTOL	116931917	2.573942658	7.3214285	2.7	12.59537116

Photon	Volume (mm^3)	Frame mass (kg)	Propulsion (kg)	Electrical pack (kg)	Total (kg)
Quadcoper	106004337.7	2.333401296	5.8571428	2.2	10.3905441
Hexacopter	111988344.6	2.465123166	8.7857142	3.1	14.35083737
Octocopter	117972348.3	2.596844964	11.7142856	4.1	18.41113056
VTOL	116931917	2.573942658	7.3214285	2.7	12.59537116

Thruster range table

Propeller	Mass (kg)	Force (N)	Safe range (km)	Operational range (km)
Quadcopter	5.733401296	56.098	0 - 9.5297	unfeasible
Hexacopter	7.365123166	72.044	0 - 7.4055	unfeasible
Octocopter	9.096844964	89.028	0 - 10.368	unfeasible
VTOL	6.773942658	66.323	0 - 8.7856	unfeasible

Ion	Mass (kg)	Force (N)	Safe range (km)	Operational range (km)
Quadcopter	10.3905441	0.1056	198040+	536.9865+
Hexacopter	14.35083737	0.1584	190030+	530.1+
Octocopter	18.41113056	0.2112	186400+	526+
VTOL	12.59537116	0.1056	218040+	540.5+

PLT	Mass (kg)	Force (N)	Safe range (km)	Operational range (km)
Quadcopter	10.3905441	0.000013333332	17624000+	799.7+
Hexacopter	14.35083737	0.000019999998	16912000+	792.8+
Octocopter	18.41113056	0.000026666664	16589000+	788.7+
VTOL	12.59537116	0.000013333332	19404000+	803.2+